

Deposition and in-situ translocation of microplastics in floodplain soils

Collin Joel Weber¹, Christian Opp², Julia A Prume³, Martin Koch³, Thorbjørn Joest Andersen⁴, and Peter Chiffard⁵

¹Philipps-University Marburg, Department of Geography

²Phillips-University Marburg, Department of Geography

³Philipps-University Marburg, Department of Physics

⁴Copenhagen University

⁵Philipps-Universität Marburg

November 22, 2022

Abstract

Microplastic (MP) contamination of freshwaters and soils has become one of the major challenges within the Anthropocene. MP is transported in large quantities through river systems from land to sea. However, the question is whether there is transport only or also deposition within the system? Floodplains and their soils as part of the river system are known for their sink function for sediments, nutrients, and pollutants. The present case study analyzes the spatial distribution of large (L-MP, 2,000–1,000 μm) and medium (M-MP, 1,000–500 μm) MP particles in floodplain soils of the Lahn River (Germany). Based on a geospatial sampling concept, the MP contents in floodplain soils are investigated down to a depth of 2 meters through a holistic method approach. The analysis of the plastic particles is carried out by density separation, visual fluorescence identification, and additional ATR-FTIR analysis. In addition, grain size analyses and $^{210}\text{Pb}/^{137}\text{Cs}$ dating was performed to reconstruct the MP deposition conditions in floodplains. The results prove a spatial frequent accumulation of MP in upper floodplain soils (0–50 cm) deposited by flood dynamics since the 1960s. MP detection over the entire soil column to a depth of 2 meters and below recent (>1960) sediment accumulation indicates MP relocation and in-situ vertical transfer of mobile MP particles through natural processes (e.g., preferential flow, bioturbation). Furthermore, the role of MP as a potential marker of the Anthropocene is assessed based on the findings. This study advances our understanding of the deposition and relocation of MP at the aquatic-terrestrial interface.

Hosted file

si_weber_et_al_2021_final.docx available at <https://authorea.com/users/537253/articles/599273-deposition-and-in-situ-translocation-of-microplastics-in-floodplain-soils>

1
2
3
4
5
6
7
8
9
10
11
12
13
14
15
16
17
18

Deposition and in-situ translocation of microplastics in floodplain soils

C. J. Weber¹, C. Opp¹, J. A. Prume^{2,4}, M. Koch², T. J. Andersen³, and P. Chiffard¹

¹ Philipps-University of Marburg, Department of Geography, Germany.

² Philipps-University of Marburg, Department of Physics, Germany.

³ University of Copenhagen, Department of Geosciences and Natural Resource Management, Denmark.

⁴ Bayreuth Graduate School of Mathematical and Natural Sciences (BAYNAT), University of Bayreuth, Germany.

Corresponding author: Collin J. Weber (collin.weber@geo.uni-marburg.de)

Key Points:

- Microplastics have accumulated frequently in the upper floodplain soils deposited by flood dynamics starting in the 1960s.
- Microplastics can be relocated within floodplain soils through natural processes and reach depths up to 2 meters.
- Plastics have become part of earths geological cycle and could therefore be used as an Anthropocene marker for soils and sediments.

19 Abstract

20 Microplastic (MP) contamination of freshwaters and soils has become one of the major
21 challenges within the Anthropocene. MP is transported in large quantities through river systems
22 from land to sea. However, the question is whether there is transport only or also deposition
23 within the system? Floodplains and their soils as part of the river system are known for their sink
24 function for sediments, nutrients, and pollutants. The present case study analyzes the spatial
25 distribution of large (L-MP, 2,000–1,000 μm) and medium (M-MP, 1,000–500 μm) MP particles
26 in floodplain soils of the Lahn River (Germany). Based on a geospatial sampling concept, the
27 MP contents in floodplain soils are investigated down to a depth of 2 meters through a holistic
28 method approach. The analysis of the plastic particles is carried out by density separation, visual
29 fluorescence identification, and additional ATR-FTIR analysis. In addition, grain size analyses
30 and ^{210}Pb and ^{137}Cs dating was performed to reconstruct the MP deposition conditions in
31 floodplains. The results prove a spatial frequent accumulation of MP in upper floodplain soils
32 (0–50 cm) deposited by flood dynamics since the 1960s. MP detection over the entire soil
33 column to a depth of 2 meters and below recent (>1960) sediment accumulation indicates MP
34 relocation and in-situ vertical transfer of mobile MP particles through natural processes (e.g.,
35 preferential flow, bioturbation). Furthermore, the role of MP as a potential marker of the
36 Anthropocene is assessed based on the findings. This study advances our understanding of the
37 deposition and relocation of MP at the aquatic-terrestrial interface.

38 Plain Language Summary

39 The occurrence of plastic as a man-made material in the environment is widely known for
40 different natural areas (e.g., oceans, rivers, soils). Nevertheless, the question arises with respect
41 to the routes through which plastic is transported across the environment, especially between
42 land and sea. Therefore, the study focuses on the content of microplastics (i.e., plastic particles
43 smaller than 5 mm or, in this case, between 2 and 0.5 mm) in floodplain soils accompanying
44 rivers as main global transport routes of the plastic. Visual analysis of plastic particles
45 (microscopic) and soil parameters revealed that microplastic particles are found very widely in
46 floodplain soils. They occur at all depths between soil surface and down to 2 meters, with the
47 highest contents in the upper 50 centimeters. These upper soil sections correspond to very young
48 soil layers in deposited sediments of the river during floods since the 1960s. However, because
49 plastic particles also occur below this level and plastic has only been increasingly released into
50 the environment since the 1950s and 60s, there must be natural processes that lead to a vertical
51 displacement of the particles, which are thus to be regarded as movable in soils.

52

53

54

55

56

57

58

59 1 Introduction

60 Global plastic pollution of marine, freshwater, and terrestrial ecosystems is one of the major challenges in the
61 Anthropocene (De-la-Torre *et al.*, 2021). Rising scientific efforts have resulted in the fact that nowadays plastics and
62 microplastics (MP) can be detected in all ecosystems worldwide (Cole *et al.*, 2011; Karbalaei *et al.*, 2018; Zhang *et al.*
63 *et al.*, 2020). Those purely anthropogenic contaminants, defined as particles with shape and surface and classified
64 about their size, are an emerging threat to global ecosystems (Machado, Anderson A. de Souza *et al.*, 2018).
65 Conventionally, MP particles are plastic particles formed by polymerization (polymers) that have a size between 1
66 and 5000 μm . In addition, larger particles are called *mesoplastics* (MEP, $> 5000 \mu\text{m}$) and smaller particles
67 *nanoplastics* (NP, $> 1 \mu\text{m}$) (Andrady, 2017). The exponential growth of global plastic production since the 1950s
68 (1950: 1.7 Mt) resulted in an annual production of about 368 Mtonne in 2019 and so for more than 70 years have
69 entailed huge potential for plastics entering the environment (PlasticsEurope, 2018, 2020).

70
71 Plastics entering the environment, regardless of its size, can be broken down further and further over time by
72 physical and chemical processes (Napper & Thompson, 2019; Chamas *et al.*, 2020). A property of polymers is that
73 they decompose slowly and do not dissolve. For this reason, modeled half-life times for buried plastic particles can
74 exceed 2,500 years, showing a long residence time in the environment (Chamas *et al.*, 2020). If, despite insufficient
75 knowledge, we consider a global "plastic cycle" as comparable to a geological cycle, sooner or later all plastic
76 residues end up in the oceans (Zalasiewicz *et al.*, 2016). Plastic pollution in the marine environment has been the
77 starting point of today's research on MP since the 1970s and has also been one of the main focuses of the scientific
78 community to date (Carpenter & Smith, 1972; Hidalgo-Ruz *et al.*, 2012; Wright *et al.*, 2013). Nevertheless, the
79 question arises regarding how plastic residues reach the oceans. Because global plastic flows, rivers, and freshwater
80 systems play an important role regarding the land-to-sea transport (Siegfried *et al.*, 2017; Alimi *et al.*, 2018;
81 Lechthaler *et al.*, 2020), it is estimated that up to 91% of the global plastic waste entering the environment could be
82 transported by rivers (Lechthaler *et al.*, 2020). Although these findings are models, the quantification of plastic loads
83 in small to large rivers illustrates that most plastics can be found there. This assumption is supported by the fact that
84 a large proportion of global plastic is produced and consumed further away from oceans (Barnes *et al.*, 2009; Ellen
85 MacArthur Foundation, 2017). However, freshwater systems cannot be regarded as transport routes only. Going
86 back to the idea of a global plastic cycle as pendant to geological cycles, temporary deposition of e.g., sediments in
87 river systems is known. This concerns especially floodplains as the surrounding areas of rivers in their
88 morphological transfer zone and part of the river system. Build up from fluvial deposits, which are also known
89 exactly to be temporary sinks for sediments (Bridge, 2003; Brierley & Fryirs, 2007; Fryirs & Brierley, 2013).

90
91 Floodplains are important ecosystems and natural habitats. They have important functions for the water balance
92 (flood retention, groundwater recharge), and they are the connecting space between the river and its catchment. They
93 are also the drainage system of landscapes (Bridge, 2003). They join and follow the river through various
94 landscapes, like geological bedrocks, and are known as important deposition and accumulation sites for fluvial
95 sediments, nutrients, and pollutants (e.g., heavy metals) (Opp *et al.*, 1993, Kalias *et al.*, 2003; Houben, 2012; Fryirs
96 & Brierley, 2013; Martin, 2019). Floodplains are a transition zone between fluvial and terrestrial environmental
97 systems, resulting in the formation of semiterrestrial floodplain soils. In addition, they have an important function
98 for humans in several parts of the world in that they have suitable conditions for agricultural use and are often
99 subject to intensive cultivation (Blettler *et al.*, 2017; Scheurer & Bigalke, 2018). The worldwide floodplain area
100 consists only of 0.61% of the total terrestrial continental area, which accounts for approximately 806,525 km^2 in
101 Europe (Nardi *et al.*, 2019). In a national comparison, the floodplain areas of rivers with a catchment area $> 1,000$
102 km^2 , accounting for around 4.4% of the national area in Germany (Bundesministerium für Umwelt, Naturschutz und
103 Reaktorsicherheit, 2009).

104
105 In contrast to the scope of research in the field of freshwater systems, the number of studies on microplastics in
106 floodplains and floodplain soils is still very limited, with only three studies focusing on the quantification of MP
107 concentrations within floodplain soils. In principle, Scheurer and Bigalke (2018) were able to show, based on the
108 example of Swiss floodplain soils, that MPs are found in 90% of the investigated soils and that the amount of MPs
109 found (0 to 55.5 mg kg^{-1}) is clearly related to the population density of the respective river catchment. Another study
110 from 2020 was able to show, using the example of the floodplains of the River Inde (North Rhine, Westphalia), that
111 microplastic contents increase with increasing flow length, particularly with respect to sliding slopes of meandering
112 bends that act as microplastic hotspots (Lechthaler *et al.*, 2021). Furthermore, a first reconstruction of the floodplain
113 chronology based on MP was achieved within this study. However, both studies focus on riparian soil areas and do

114 not consider any or restricted depths under 5 cm (Scheurer & Bigalke, 2018) or 110 cm at riparian sites and slopes
 115 (Lechthaler *et al.*, 2021). Considering floodplain soils as a potential temporary sink for microplastics, this
 116 explorative view is insufficient but understandable because of the early stage of the research field. For a spatial
 117 quantification and a deeper understanding of the deposition processes of MPs within floodplain systems and soils,
 118 more systematic studies, in contrast to the established “explorative studies” in the field of soil science, are required
 119 (Weber *et al.*, 2020). The third study, which is a preliminary study to the one presented here, showed that MEP and
 120 coarse microplastics (CMP, > 2,000 μm) with average loads of 2.06 p kg^{-1} ($\pm 1.55 \text{ p kg}^{-1}$) and 1.88 p kg^{-1} ($\pm 1.49 \text{ p kg}^{-1}$)
 121 are widespread, but are spatial heterogenous distributed in floodplain soils, down to depths between 75 and 100
 122 cm (Weber & Opp, 2020). MEP and CMP particles reaching those depths within floodplain soils indicate that not
 123 only depositional processes but also in-situ vertical transfer takes place within these soils (Weber & Opp, 2020).

124
 125 The current state of research proves that plastics and MPs are present in floodplain soils and that these soils can be
 126 considered a potential temporal sink for MP. However, input processes like the deposition by flood dynamics or
 127 other sources, as well as the mobility of introduced and deposited MP within floodplain soils, still remains unclear.
 128 Both questions are of particular relevance, however, given that plastics in soils are an increasing threat to terrestrial
 129 ecosystems. Previous studies suggest a wide range of impacts of MP on soil properties (physical and chemical), soil
 130 organisms, and plant growth (Huerta Lwanga *et al.*, 2017; Rillig *et al.*, 2017; Hüffer *et al.*, 2019; Zhang *et al.*,
 131 2019). Moreover, 95% of global food production is obtained directly or indirectly from soils (Food and Agriculture
 132 Organization of the United Nations [FAO], 2015). If soils are vulnerable to plastic, and if initial evidence shows that
 133 MP can also enter the food chain and the human body, the consequences for global food security and the ecological
 134 state of soils will be unacceptable for the society in the Anthropocene (Lahive *et al.*, 2019; Rillig *et al.*, 2019;
 135 Selonen *et al.*, 2020; Ragusa *et al.*, 2021).

136
 137 This paper aims to improve the understanding of the deposition and potential in-situ transport of MP in floodplain
 138 soils on the basis of a geospatial research approach with respect to landscape characteristics and a holistic method
 139 approach. The present study focuses on the quantification and spatial distribution of large MP (L-MP, 2,000-1,000
 140 μm) and medium MP (M-MP, 1,000–500 μm) because particle size is the decisive factor in determining deposition
 141 properties and potential mobility within floodplain soils (Kooi & Koelmans, 2019; Waldschläger & Schüttrumpf,
 142 2019a).

143
 144 Based on a holistic research approach containing preceding sampling site selection and systematic soilscape survey,
 145 analyses of MP, physical soil properties, and recent sediment dating, the following key issues should be addressed:
 146 (1) Which concentrations of L-MP and M-MP occur in floodplain soils? (2) Is it possible to trace the lateral and
 147 vertical spatial distributions of MP back to a specific environmental driver (e.g., land-use or flood dynamics)? (3)
 148 Can the conditions and processes of MP deposition in floodplain systems be reconstructed with the use of MP as a
 149 stratigraphic marker? This is intended to achieve the goal of an improved understanding of the spatial dynamics of
 150 MP within the three-dimensional system of floodplain soils and to enable targeted research on responsible processes
 151 for MP distribution in floodplain systems. In addition, the role of MP in the sedimentary budget and the geological
 152 cycle of the Anthropocene will be assessed on the basis of the questions presented.

153 **2 Materials and Methods**

154 **2.1 Study Area**

155 The implementation of a geospatial sampling approach took place within the floodplain area of the Lahn River
 156 (Hesse, Germany). The Lahn River, with a total length of 245.6 km and a catchment area of 5,924 km², is located
 157 within the central German low mountain range (Figure S1) (Regional Council Giessen, 2015; Meschede & Warr,
 158 2019). Based on catchment geology, resulting landscape properties, and hydrology, the Lahn valley consists of
 159 different zones: (A) upper course (Rhenish Slate Mountains, smaller floodplain), (B) middle course (a sequence with
 160 wide, basin-like and narrow valleys with changing wide and narrow floodplains), (C) narrow valley (almost without
 161 distinctive floodplain), and (D) lower course with individual valley widenings and floodplains (Weber & Opp,
 162 2020). The upper floodplain sediments and soils within the Lahn River floodplain are formed by the deposition of
 163 organic-rich silt and loams during the late Holocene and latest Pleistocene on older Pleistocene gravel and sand
 164 deposits (Rittweger, 2000; Bos & Urz, 2003). The floodplain soils within the direct surrounding area of the Lahn
 165 River comprise a total area of 88.9 km² within the federal state of Hesse. Major soil types are Fluvisols (70.7 km²),

166 Gleyic Fluvisols (6.2 km²), Fluvic Gleysols (2.7 km²), and Stagnic Fluvisols (6.4 km²) (Hessian Agency for Nature
167 Conservation, Environment and Geology, 2020).

168 The Lahn River valley is subject to frequent flood events, despite of the anthropogenic changes like partwise
169 canalization or river conversions in the case of flood management measures (Gleim & Opp, 2004). Even if very
170 strong floods, such as the widespread medieval flood events (e.g., 1255, 1552) have become rarer, the last century's
171 high-flood event occurred only 37 (1984) years ago (Gleim & Opp, 2004). Therefore, a steady record of sediment
172 deposition and local bank erosions through floods can also be observed in the present (Martin, 2015, 2019). The
173 investigated floodplain soils are partwise under agricultural usage (crop- or grassland), except for riparian strips and
174 settlements. In general, the Lahn River catchment could be named called rural, with only 8.4% of strong
175 anthropogenic land use (urban, traffic, industry) and a population density of 266 inhabitants per km² (Regional
176 Council Giessen, 2015). Urban parts are restricted to four medium-sized cities along the river course (Martin, 2012).

177 2.2 Geospatial Sampling Approach

178 For a deeper understanding of the spatial dynamics of microplastics in floodplain soils, systematic studies with a
179 focus on spatial representativeness in contrast to established explorative studies are required (Weber *et al.*, 2020). A
180 first introduction of the approach presented here was made by Weber and Opp (2020), following the suggestions of
181 Weber *et al.* (2020) and Weihrauch (2019). The common approach in environmental science studies soils and
182 microplastics within soils at individual sites (e.g., independent profiles, topsoil samples) without a wider spatial
183 context as a result of logistical limitations. However, many key processes for soil formation act not only locally but
184 in the context of a wider landscape (Weihrauch, 2019; Weber *et al.*, 2020). The soils in floodplain areas are
185 especially the result of processes and, despite anthropogenic influence, are subject to processes that not only are
186 local but also affect the entire floodplain and are significantly determined by river systems, catchment sections, or
187 the entire catchment. To record and study the environmental processes and drivers that are responsible for the
188 distribution and spread of microplastic in floodplain soils, it is necessary to consider a larger part of the landscape.
189 Floodplain soils have to be understood as part of a landscape in which environmental processes take place and thus
190 as part of a "soilscape" (Willgoose, 2018). In the case of the floodplain soils studied here, and with regard to
191 microplastic pollution, various processes such as flooding, groundwater recharge, or land use are important because
192 they could have an influence on the deposition, accumulation, and mobility of plastic particles in the soils itself. To
193 understand these processes, not only on a soil profile itself but also in the spatial context of the floodplain landscape
194 and its soilscape, a geospatial approach was applied to identify suitable and representative sampling sites. Each
195 sampling site must therefore be representative for a larger part of the river area (Lahn River zones, Chapter 2.1) and
196 its floodplain in the case of soil formation, morphology, flood dynamics, and land use.

197
198 To identify suitable sampling sites within in the floodplain landscape of the Lahn River, the following criteria were
199 set: (1) location within a natural flood retention area with potential for frequent flood events (recent), (2) Extended
200 floodplain area with a sequence of different morphological units and soil differentiation, (3) land use differences in
201 floodplain cross-section and undisturbed floodplain cross-section (e.g., no railway dams), and (4) no direct potential
202 anthropogenic MP source like highways or industrial sites (Weber & Opp, 2020).

203
204 After identifying suitable sampling sites and an initial soil mapping to obtain an overview on soilscape properties,
205 four floodplain cross-section transects were selected that are representative of a larger floodplain area with
206 comparable soil properties (same locations as Weber & Opp, 2020). The transect sites corresponded to the valley
207 sections A: site ELM; B: site ROT and STD; and D: site LIM (Chapter 2.1). At each transect, two sampling plots
208 (ELM, ROT) or four sampling plots (STD, LIM) were established between the river bank and the floodplain edge
209 (Figure S2). Two soil profiles with a distance of 5 m to each other were drilled to a depth of 2 m via pile core
210 driving (100 mm and 80 mm core diameter) and sampled according the following depth sections: 10 cm sections
211 (for 0–0.5 m), 25 cm sections (for 0.5–1.5 m), and 50 cm sections (for 1.5–2.0 m). Sample material with an average
212 sample mass of 1150 g (in total 120 samples, 111 for MP analyses) (Figure S3) was transported in cornstarch
213 bioplastic bags (Mater-Bi bags, Bio Futura B.V., Rotterdam, Netherlands). The comparatively large amount of
214 sample material was taken because previous studies have shown very heterogeneous occurrences of microplastics in
215 soils (Liu *et al.*, 2018; Scheurer & Bigalke, 2018; Corradini *et al.*, 2019). Soil samples for dating were taken at the
216 transect sites ELM (upper course, section A, core ELM-D) and LIM (lower course, section D, core LIM-D) at the
217 beginning of the plain floodplain (behind the riverbank, not under landuse). For this purpose, a drill core (80 mm, 1
218 m depth) was drilled and then excavated to obtain a drill core free of disturbances as far as possible. The core was
219 subsequently divided into 2 cm sections, which were collected in the field and transported in PE-bags. In this way,

220 42 samples from core ELM-D (0–84 cm soil depth) and 45 samples from core LIM-D (0–90 cm soil depth) could be
221 obtained.
222 Stratigraphy and pedogenesis of each soil profile were documented according the German soil classification (Ad-
223 hoc AG Boden, 2005), the FAO Guidelines for soil description (FAO, 2006), and the WRB 2015 (IUSS Working
224 Group, 2015). Soil properties (horizon sequences) and soil type according to WRB are documented in Table T1
225 (Supplementary). Contamination prevention during sampling process was performed by avoiding plastic tools and
226 using stainless-steel spatula, steel drill equipment, and bioplastic bags.

227 2.3 Sample Preparation, Soil Analyses, and Dating

228 Sample preparation followed the sample preprocessing process introduced by Weber and Opp (2020) for the
229 analysis of MEP and CMP. Basically, the sample preprocessing was carried out without using plastic tools or
230 materials (including cotton lab coats) and by reducing the exposition time for each sample as much as possible to
231 avoid air contaminations. Soil samples for microplastic analyses were transported in cornstarch bags and dried at
232 45°C in a drying chamber for a maximum of 4 days. Subsequently, the samples were carefully mortared to solve soil
233 macroaggregates because microplastics can be attached within those aggregates (Zhang & Liu, 2018). This process
234 was carried out manually to ensure a careful dissolution of the macroaggregates with minimum impact on plastic
235 particles. Afterwards, the sample material was dry sieved according to the size classes of MEP (> 5,000 µm), CMP
236 (> 2,000 µm), and MP (< 2,000 µm) through stainless-steel sieves (Retsch, Haan, Germany). During the sieving
237 process, sieves were covered with stainless-steel plates. To homogenize the sample and simultaneously obtain a
238 representative subsample (approx. 12.5 % of total sample volume) for standard soil analyses, the sample was divided
239 by means of a rotary sampler (Retsch, Haan, Germany). Each size fraction and subsample was afterwards weighed
240 and stored in fresh cornstarch bags.

241
242 Soil samples for dating purposes were processed in a comparable manner: The samples were transported in PE-bags,
243 weighed wet, and then dried at 50°C in a drying chamber for 4 days. Afterwards, they were ground and sieved to 2
244 mm through stainless-steel sieves. The coarse soil fraction (> 2 mm) and the fine soil fraction (< 2 mm) were dry
245 weighed. A subsample (approx. 27 g of fine soil material each) was placed in 50 mL PE-containers and sent to the
246 laboratory for further analyses. Soil moisture, coarse soil fraction, and soil density was calculated.

247
248 Standard soil analyses included the determination of organic matter (OM) and texture analyses. The content of OM
249 was measured by loss of ignition (DIN ISO 19684-3:2000-08). Soil texture was determined for each sample with the
250 Integral Suspension Pressure Method (Durner *et al.*, 2017) after samples had been prepared according to DIN ISO
251 11277:2002–08.

252
253 Samples for dating purpose were analyzed at the Gamma Dating Center, Department of Geosciences and Natural
254 Resource Management, University of Copenhagen for measurements of the activity of ²¹⁰Pb and ¹³⁷Cs via gamma
255 spectrometry. The measurements were carried out on a Canberra ultralow-background Ge-detector. ²¹⁰Pb was
256 measured via its gamma-peak at 46.5 keV, ²²⁶Ra via the granddaughter ²¹⁴Pb (peaks at 295 and 352 keV), and ¹³⁷Cs
257 via its peak at 661 keV. The chronologies were calculated using a constant rate of supply (CRS) model in which the
258 activity in the lower portion of the cores was calculated on the basis of a regression of the activity of unsupported
259 ²¹⁰Pb versus cumulated mass depth (Appleby, 2001; Andersen, 2017).

260 2.4 Microplastic Analyses

261 Presented analyses of microplastic particles within floodplain soils consisted of a three-step procedure: (1)
262 separation, (2) staining, and (3) identification. Because soil is an environmental medium containing different
263 materials or substances, the major components, namely (a) mineral component and (b) organic component, must be
264 separated from the searched component, (c) microplastics (Hurley *et al.*, 2018; Möller *et al.*, 2020; Ruggero *et al.*,
265 2020; Thomas *et al.*, 2020).

266
267 Separation of mineral components was performed within the “MicroPlastic Sediment Separator” (MPSS) (Hydro-
268 Bios Apparatebau GmbH, Kiel-Altenholz, Germany) as a separation unit and the only commercially available. The
269 advantage of handling a large amount of sample against the background of a heterogeneous distribution and
270 unknown concentrations of plastic particles in the environment must be highlighted at this point, as should the
271 disadvantage of a long separation time due to the size of the device (Standpipe). Based on the principle of density

272 separation, organic sample components and the searched plastic can rise through the comparable material density
273 within the unit, while mineral components remain at the bottom (Imhof *et al.*, 2012). Recovery rates of the MPSS
274 are estimated with 100% for CMP and large MP (> 1 mm) and 95% for smaller MP (1,000–40 µm) (Imhof *et al.*,
275 2012). Potential plastic contaminants (e.g., room air) were controlled by blank samples (Stock *et al.*, 2019). In a total
276 of five blanks (during 41 MPSS runs with a maximum of three instruments), 7 potential plastic particles (fragments
277 and filaments) with a mean size of 341.28 µm were found. Because of their size, visual identification of the particles
278 was not possible through ATR-FTIR.

279
280 The MPSS unit was filled with a sodium chloride (NaCl) solution, density adjusted to approximately 1.2 g/ml and
281 sieved with a 300 µm stainless-steel sieve. Solution density was controlled before and after separation process via
282 pipetting and weighing, along with the help of an aerometer (Figure S3). With revolving rotor, sample material was
283 added, and the MPSS unit was closed (dividing chamber). The rotor was left running for 60 minutes, and separation
284 process left for another 14 hours (Imhof *et al.*, 2012). After separation time, the integrated ball valve was closed and
285 the dividing chamber was removed to allow the separated material to be rinsed into glass beakers using filtered (<
286 300 µm) NaCl solution. After the separation process, the remaining sample material was separated into the
287 following size classes using stainless-steel sieves (Ø 75 mm, Atechnik, Leinburg, Germany) and deionized water: >
288 1,000 µm (L-MP), > 500 µm (M-MP), and 500 to 50 µm (S-MP). After sieving, the sieve residues were filtered on
289 pleated cellulose filters (LLG-Labware, Meckenheim, Germany) and for S-MP via vacuum filtration on round
290 cellulose filters (LLG-Labware, Meckenheim, Germany). The S-MP fraction was saved for later analyses, currently
291 in progress.

292
293 To separate the remaining sample material of organic material and potential plastic particles in L-MP and M-MP
294 fraction, a Nile Red staining procedure and visual fluorescence identification was applied (Maes *et al.*, 2017; Konde
295 *et al.*, 2020). Following the suggestions of Konde *et al.* (2020) a Nile Red solution with a concentration of 20 µg/mL
296 Nile Red (Sigma-Aldrich, Taufkirchen, Germany) solved in an ethanol-acetone (1:1) mixture was dropped on each
297 filter, using a pipette and subsequently sprayed on (using a spray bottle). The initial dropping prevents the loss of
298 particles due to the subsequent spraying with uniform coverage of all particles on the filter. Filters were stained for
299 10 minutes at 50°C within a drying chamber before visual analyses (Konde *et al.*, 2020). Stained filters were
300 afterwards visual detected under a stereomicroscope (SMZ 161 TL, Motic, Hong Kong) with fluorescence setup
301 (Excitation: 465 nm LED; Emissions 530 nm color long pass filter: Thorlabs, Bergkirchen, Germany) (Konde *et al.*,
302 2020). Filters were detected systematically to observe the entire filter surface under fluorescent and white light
303 (Figure S4 and S5). Each fluorescent particle and other potential plastic particles (matching the criteria according to
304 Norén, 2007) were collected and stored in microplates (Brand, Wertheim, Germany). Potential plastic particles were
305 classified according to surface characteristics, which were photographed (Moticam 2, Motic, Hong Kong) and
306 measured (Motic Images Plus 3.0, Motic, Hong Kong).

307
308 For final identification and to avoid overestimations, each potential plastic particle was analyzed with a Tensor 37
309 FTIR spectrometer (Bruker Optics, Ettlingen, Germany) combined with a Platinum-ATR-unit (Bruker Optics,
310 Ettlingen, Germany). In some cases, adherent soil or organic material was removed with stainless-steel tweezers.
311 The Platinum-ATR-unit was cleaned with 2-propanol (CH₃CHOHCH₃) between each measurement. Measurement
312 was performed with 20 background scans followed by 20 sample scans for each sample (Jung *et al.*, 2018). Spectral
313 resolution was set to 4 cm⁻¹ in a wavenumber range from 4,000 cm⁻¹ to 400 cm⁻¹ (Primpke *et al.*, 2017; Primpke *et*
314 *al.*, 2018).

315 2.4.1 Limitations and insecurities

316 Despite the continuous development of analytical methods for microplastics in soils, no standardized method has
317 been established to date (Bläsing & Amelung, 2018; Möller *et al.*, 2020). The present work focuses on the
318 combination and adaptation of methodological approaches already presented. First, in the case of density separation
319 within the MPSS unit, the recovery rates were reported to be > 95% for particles down to 40 µm in size by the
320 developers (Imhof *et al.*, 2012). However, the construction and size of the device involves considerable time and
321 expense, which is only profitable when larger sample volumes are used (Coppock *et al.*, 2017). In contrast to other
322 concentrated salt solutions (e.g., ZnCl₂), the flotation medium that was used (NaCl) is cost effective and
323 environmentally friendly (Coppock *et al.*, 2017). A limitation arises from the fact that only plastic particles with a
324 density of < 1.2 g/ml can be separated. Common polymer types such as Polyethylene terephthalate (PET) or
325 Polyvinyl chloride (PVC) may not be separated. Second, concern regarding the Nile Red staining procedure and

326 recovery rates up to 96.6% from spiked marine sediments in combination with density separation are documented
327 (Maes *et al.*, 2017). In contrast to other methods such as the oxidation of organic matter (e.g., by acid digestion),
328 Nile Red staining offers a completely particle-preserving approach. Depending on the surface of organic material,
329 but especially on calcium-containing shells (e.g., isolated freshwater mussels in alluvial sediments), Nile Red can
330 also bind these materials and thus hinder the visual distinction between plastic and non-plastic (Konde *et al.*, 2020).
331 From 225 selected particles during the Nile Red staining procedure, 46 particles were too small for ATR-FTIR
332 analysis (> 300 μm , adherent to organic components); and of 179 analyzed samples, 21 particles (11.73 %) were
333 classified as natural (non-plastic) material. This limitation can and must be lifted by (a) systematic examination of
334 the sample under fluorescent and white light, (b) collection of all potential particles, and (c) a subsequent
335 identification of the particles using analytical methods such as ATR-FTIR to prevent overestimation. Because the
336 application of an FTIR with ATR unit (like Tensor 37, Bruker Optics, Ettlingen, Germany) is carried out by hand
337 only, particles smaller than 500 μm or 300 μm should not be investigated because they are difficult to handle and as
338 the sample and because ATR crystal often have insufficient contact area. Furthermore, in the case of heavily
339 degraded and weathered particles, there may be no match with different spectral databases because the quality of the
340 spectra is insufficient (Primpke *et al.*, 2018).

341 2.5 Data and Statistical Analyses

342 Data processing of FTIR spectra was performed in OPUS 7.0 (Bruker Optics, Ettlingen, Germany) and Spectragryph
343 (Version 1.2.14; Menges, 2020; Oberstdorf, Germany). Spectra identification and polymer type assignment was
344 carried out according to a previously defined scheme (Figure S6). Because the available OPUS database (OPUS 7.0
345 internal database) contains only insufficient entries of plastic products (only industrial polymers) and no entries of
346 environmental materials, the following procedure was performed with each spectrum: Particles with a identification
347 hit quality higher than 700 within OPUS 7.0 was counted as identified polymer type or group. In the case of
348 particles that show an identification hit quality between 700 and 300, the absorption bands were manually checked
349 for polymer identification according to the criteria of Jung *et al.* (2018). If a sufficient identification of absorption
350 bands were possible, then the particles were also counted as identified polymer type or group (Jung *et al.*, 2018).
351 Spectra of particles with a hit quality less than 300, as a limit for satisfactory identification (Primpke *et al.*, 2017;
352 Lorenzo-Navarro *et al.*, 2018; Primpke *et al.*, 2018), were automatically compared with spectra databases for natural
353 materials provided by Spectragryph (Kimmel_Center: Collection of 363 FTIR absorbance of natural and biogenic
354 material of archeological interest. Provided by S. Weiner from Kimmel Center for Archaeological Science,
355 Weizmann Institute of Science, Israel). In the case of no match in both cases, the spectra were finally matched with
356 the database of "Open Specy" (Cowger *et al.*, 2020). In this case, a satisfactory match was always achieved. In case
357 of a match with natural or biogenic material, potential plastic particles were counted as natural material and
358 excluded from further analyses.

359
360 Basic statistical operations were performed in Microsoft Excel 2013 (Microsoft; Redmond, WA, USA), in R (R
361 Core Team, 2020), and RStudio (Version 3.4.1; RStudio Inc.; Boston, MA, USA). Data visualization, tests for
362 normal distribution (Shapiro-Wilk), linear regression analyses, Pearson or Spearman correlation analyses, and
363 variance analyses (ANOVA) were conducted with the standard R-packages and "graphics," "stats," "vioplot,"
364 "ggplot2," "ggridges," and "scatterplot3d." We interpreted statistical analysis results as significant with a p-value <
365 0.05.

366 3 Results and Discussion

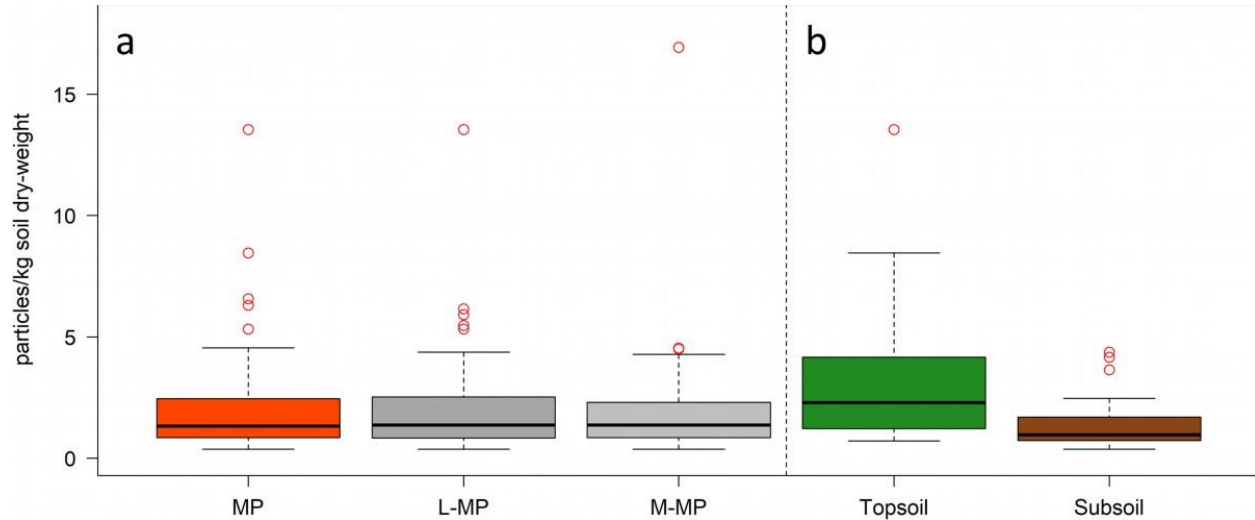
368 3.1 Microplastics and their characteristics in floodplain soils

369 In total, 149 particles from 111 soil samples could be successfully and clearly identified as plastic particles. There is
370 a positive rate (plastic containing samples) of 71.2% within the samples from topsoils down to 2 m deep soil layers.
371 Nile Red staining shows a false positive rate of approximate 12.0 %. However, even if only the definitely identified
372 particles are used for further data evaluation, it should be clear that in all cases the lower range of the actual plastic
373 pollution is concerned. The identified particles result in average plastic concentrations of 2.14 mp/kg⁻¹ (number of
374 particles in particle size class per soil dry weight), composed from 2.13 L-mp/kg⁻¹ and 1.91 M-mp/kg⁻¹ (Figure 1a).
375 With the exception of the plastic-free samples (28.8 %), the values vary between 0.37 mp/kg⁻¹ up to 13.54 mp/kg⁻¹
376 for the entire MP amount, with absolute maximum value of 16.93 M-mp/kg⁻¹ including MEP and CMP amount from
377 the preliminary study (Weber & Opp, 2020). In comparison to other studies that reported the MP concentrations for

378 soils by particle/per kg, the concentrations found are clearly below those in agricultural topsoils (Liu *et al.*, 2018;
 379 Zhang & Liu, 2018; Corradini *et al.*, 2019). A sufficient comparison with the first study on microplastics in
 380 floodplain topsoils, reported for Swiss nature reserves by Scheurer and Bigalke (2018), is not feasible because of the
 381 different used units (mg/kg). In the case of the investigation of bank profiles and topsoils of the Inde River (North
 382 Rhine-Westphalia) by Lechthaler *et al.* (2021), the corrected average concentrations with 47.9 mp/kg⁻¹ (depth
 383 profiles) and 25.4 mp/kg⁻¹ (surface samples) also exceed those available here.

384
 385 Comparable to the results for larger plastic particles (MEP, CMP) (Weber & Opp, 2020) and to the work of
 386 Lechthaler *et al.* (2021), the contents in topsoil (0–30 cm) are clearly above those in subsoil (30–200 cm) (Figure
 387 1b). Average values of 3.33 mp/kg⁻¹ in topsoils and 1.34 mp/kg⁻¹ in subsoils are significantly different (p-value =
 388 0.0002).

389



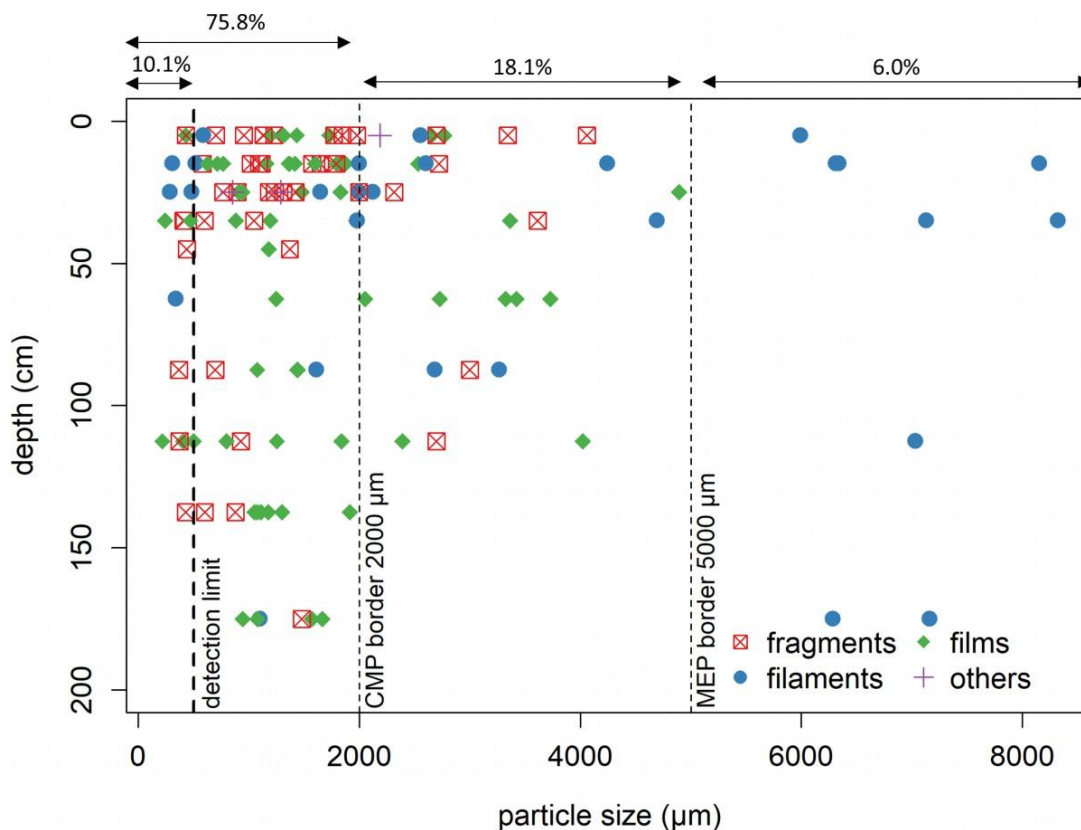
390

391

392 **Figure 1.** Overview of microplastic concentrations in floodplain soils. (a) Concentrations auf total microplastics
 393 (2,000–500 μm , MP), large microplastics (2,000–1,000 μm , L-MP), and medium microplastics (1,000–500 μm , M-
 394 MP) given in particles (p) per kg soil dry-weight. (b) Concentrations of total microplastics (2,000–500 μm , MP)
 395 within topsoil (related soil A-horizon, depth: 5 to max. 30 cm) and subsoils given in particles (MP) per kg soil dry
 396 weight.

397

398



399
400

Figure 2. Depth distribution of plastic particles and size classified by plastic shape, including size borders of the ATR-FTIR detection limit (500 μm), CMP (2,000 μm) border, and MEP (5,000 μm) border.

403

404 Particle size ranges between 219 μm to 8,321 μm , with an average of 1,171 μm ($n = 149$) for identified particles.
405 Therefore, 10.1% of all ATR-FTIR-analyzed particles were smaller than the fixed detection limit of 500 μm (Figure
406 2). Major share of particles size lies between the minimum value and 2,000 μm (MP to CMP border) within the
407 upper 50 cm of soil column, including fragments, films, and some filaments. Against expectations, 24.1% of
408 identified particles show a size larger than the CMP- and MEP-size border, despite the previous sieving procedure.
409 Because the longest diagonal of the particles was consistently measured, the width of these particles can be less than
410 2,000 μm . This is also clear from the fact that only filaments (measurement of filament length) occur in the size
411 range above 5,000 μm .

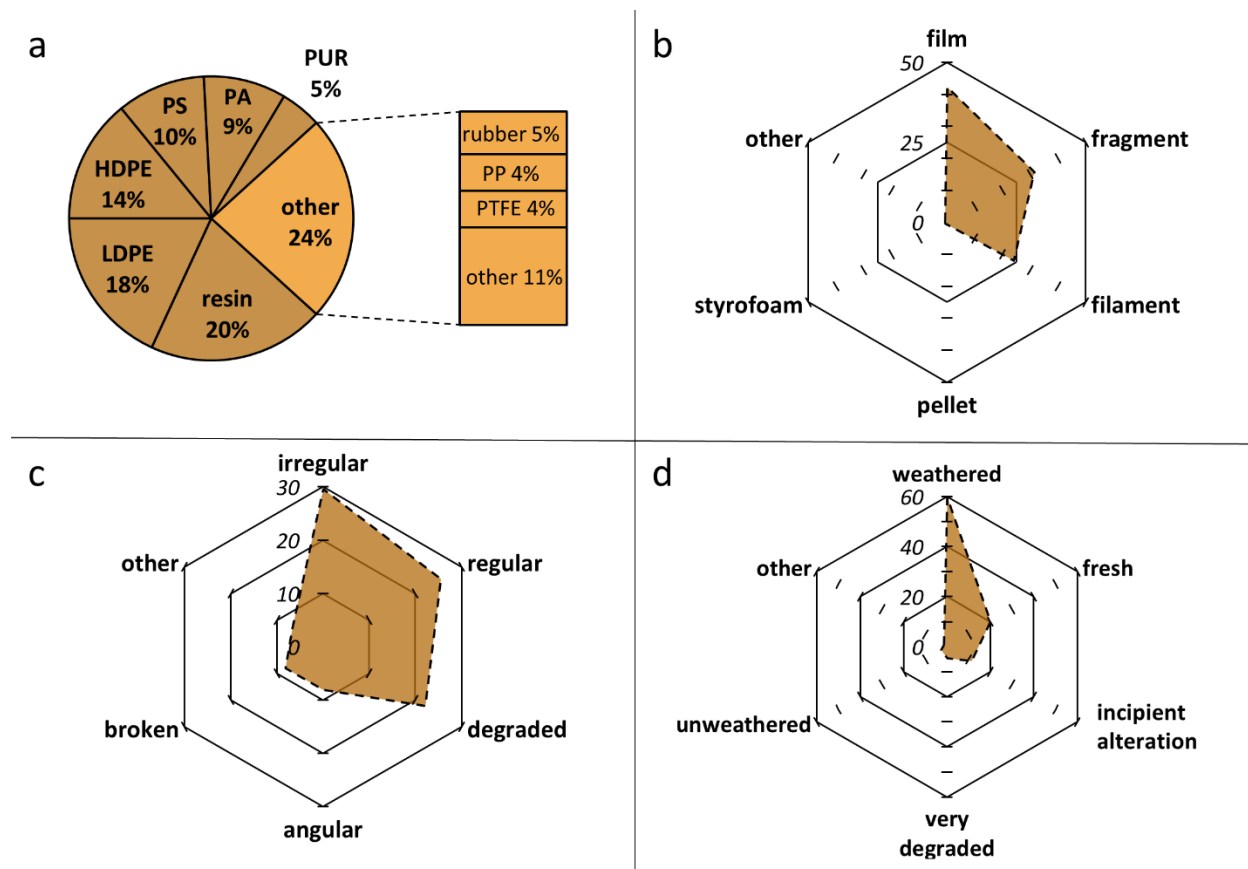
412

413 The characteristics of detected plastic particles also correspond to the findings of other studies. Major particle types
414 are films (42.3%), fragments (31.5%), and filaments (24.2%) with usually irregular or degraded shapes, except in
415 the case of filaments, which show regular surfaces (Figure 3, S7). This result clearly corresponds to the findings
416 within the Inde River catchment (Lechthaler *et al.*, 2021). More than half of all particles detected show a weathered
417 (59.7%) or incipient alteration (11.4%) surface according to visual criteria, whereas fresh surfaces occur for 20.1%
418 of all particles.

419

420 Typical polymer types like low-density polyethylene (LDPE) or high-density polyethylene (HDPE), polystyrene
421 (PS), and polyamides (PA, including Nylon-6) could be identified by ATR-FTIR analysis. The results correspond to
422 the most frequently produced and used plastics in Europe (PlasticsEurope, 2018). One surprising finding was the
423 high number (20.1%) of resins (synthetic or polymer resins, grouped as resins) in contrast to other current studies on
424 microplastic in soils (Liu *et al.*, 2018; Piehl *et al.*, 2018; Scheurer & Bigalke, 2018; Zhang & Liu, 2018; Corradini *et al.*,
425 2019; Lechthaler *et al.*, 2021). The particles classified as “resins” could be significantly identified only by the
426 OpenSpecy database. The resin entries contained in the database are from Primpke *et al.* (2018) and include
427 epoxides, polyurethane acrylic, phenoxy, and polyamide resins, which explains the frequent assignment in OPUS
428 7.0 to PA (with low hit quality). In principle, however, having resins as the largest group of plastic types is plausible

429 because these are used in countless objects, and nonfiber plastics contain 97% polymer resins in addition to other
 430 additives (7%) (Zink *et al.*, 2018).
 431

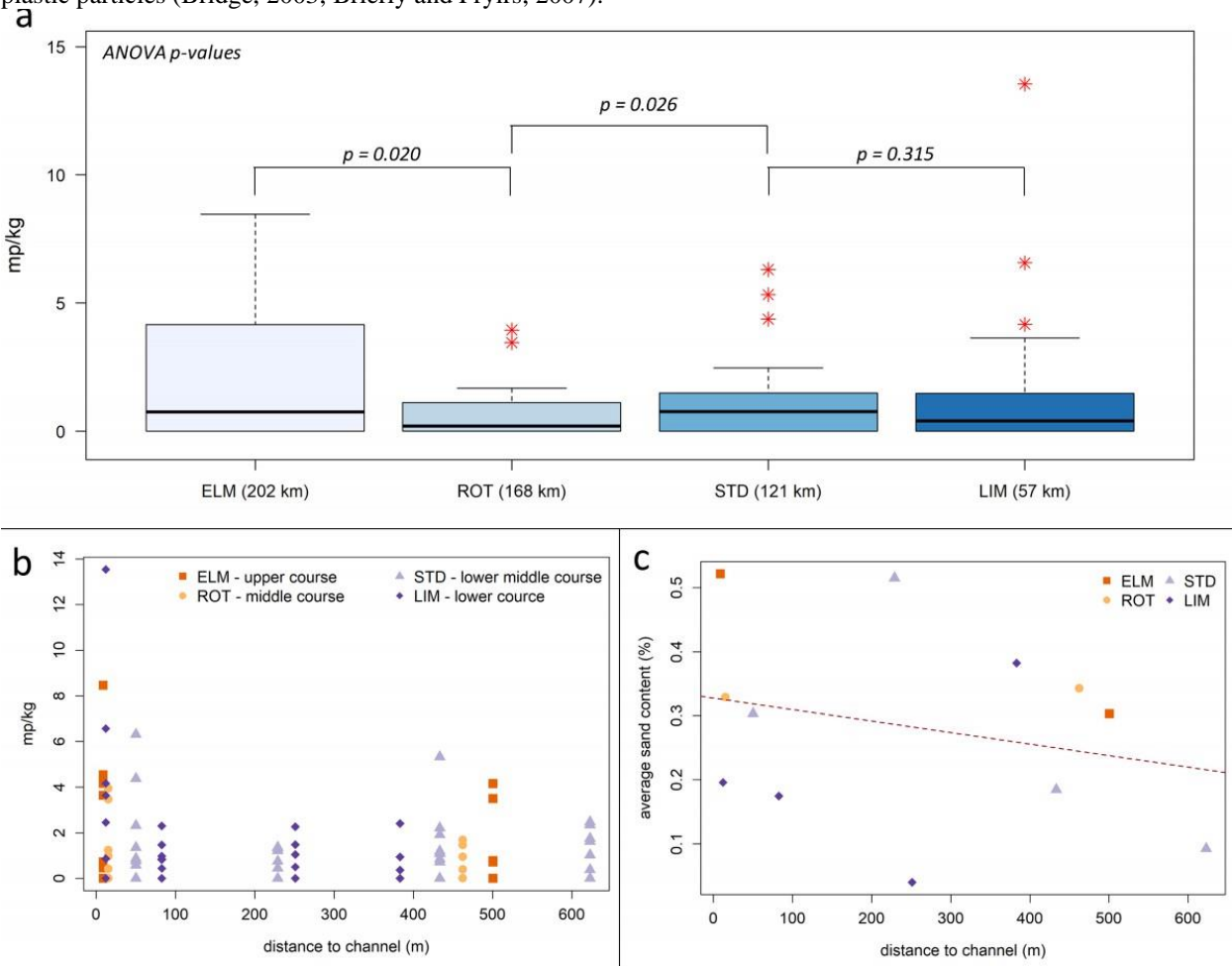


432
 433
 434
 435 **Figure 3:** Microplastic particle characteristics. (a) Identified polymer types through ATR-FTIR analyses (class other
 436 includes polymers such as PET, CSM, ABS). (b) Percentage share of particle types. (c) Percentage share of surface
 437 forms. (d) Percentage share of surface conditions.
 438

439 3.2 Lateral microplastic distribution

440
 441 The evaluation of the lateral distribution of microplastics in floodplain soils can be conducted at two spatial scales:
 442 Level one follows the catchment scale and the course of the river (metric measure: river-km), and level two follows
 443 the floodplain cross-sections (transect sites) with increasing distance to the watercourse (metric measure: distance in
 444 m). Figure 4a shows the range of total MP concentrations at each transect site from upstream (ELM, river km: 202)
 445 to the downstream site (LIM, river km 57). Average values are significant different between site ELM and ROT, as
 446 well as ROT and STD. Median values including negative samples (zero-values) are 0.75 mp/kg⁻¹ (ELM), 0.20
 447 mp/kg⁻¹ (ROT), 0.76 mp/kg⁻¹ (STD), and 0.40 mp/kg⁻¹ (LIM). An increase along the course of the river cannot be
 448 concluded on this basis. However, except for the upper reaches (ELM), maximum MP concentrations increase
 449 continuously from STD (upper middle reaches) to LIM (lower reaches). The simple assumption of an increasing
 450 accumulation of microplastics in floodplains with increasing flow length of the river, caused by the also increasing
 451 number of potential plastic sources and available water quantity and sediments, cannot be upheld unequivocally
 452 (Scheurer & Bigalke, 2018; Xiong *et al.*, 2018; Liu *et al.*, 2019). Moreover, local phenomena, instead of a
 453 superordinate accumulation, ensure a heterogeneous distribution. Nevertheless, the significant increase in maximum

454 concentrations seems to indicate that, with increasing river length and thus reduced flow velocity and higher
 455 frequency of floods, more microplastic particles can be deposited (Bridge, 2003; Brierly and Fryirs, 2007).
 456 Regarding the lateral level two, maximum concentrations are clearly reached next to the river bank and within a
 457 short distance from the river (Figure 4b). Independent of this, a widespread distribution of plastic contents around or
 458 above the mean value of 2.14 mp/kg^{-1} can be determined for the entire study in the floodplain cross-sections.
 459 According to the general knowledge that lateral sediment deposition decreases with increasing distance from the
 460 watercourse, which is reflected in the grain size differentiation of coarse-grained sandy sediments near the channel
 461 and fine-grained (clayey) sediments at the floodplain edge, this can also be assumed for the lateral distribution of
 462 plastic particles (Bridge, 2003; Brierly and Fryirs, 2007).



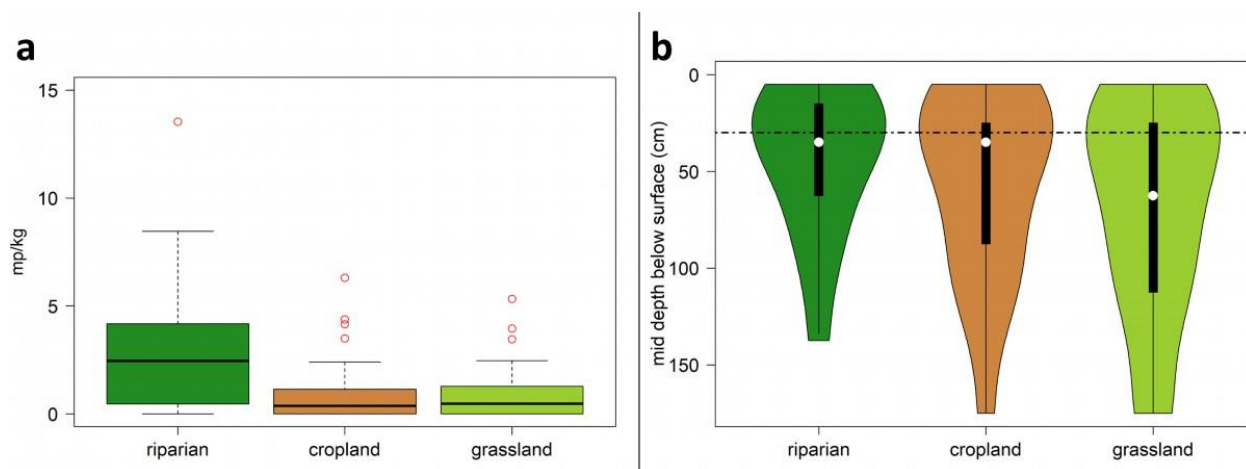
463
 464
Figure 4. Lateral microplastic distribution. (a) Lateral microplastic distribution on the catchment scale given
 466 through total MP concentrations (mp/kg) according to sampling sites (Figure S1, Chapter 2.2) and river km. (b)
 467 Total MP concentrations (mp/kg) opposite distance to channel (m) at each sampling point classified according the
 468 four sampling sites. (c) Average sand content (%) opposite distance to channel (m) at each sampling point classified
 469 according the four sampling sites.

470
 471 Figure 4c illustrates the average sand concentration within the upper 50 cm soil at each sampling point. Because the
 472 upper 50 cm of the floodplain soils contain the most microplastics (see Figure 2 and Chapter 3.3), the average sand
 473 content can provide information about the lateral deposition dynamics. With the exception of the ROT transect, the
 474 sand content of all transects decreases significantly with distance from the river. Outliers in the STD and LIM
 475 transects are due to the location of the points in a flow channel (STD-2, younger sandy flow channel deposits) and
 476 the over-deposition by slope erosion at the floodplain edge of the LIM transect (LIM-4). This results in a slight
 477 linear relationship between sand contents and distance ($R^2 = 0.126$, $p = 0.002$). The highest contents (maxima) are
 478 thus reached where the sand contents at transect level are also highest (near water bodies like river banks). Even

479 though the sedimentation and erosion properties of plastic particles differ from those of the sediment (Waldschläger
 480 & Schüttrumpf, 2019b), the question arises as to how this spatial distribution pattern is formed. In the area close to
 481 the watercourse (proximal floodplain), where increased deposition of sands take place, flow velocities should be
 482 significantly higher during floods as in the floodplain edge area (distal floodplain), where the reduced velocities
 483 (caused by higher terrain roughness) result in the deposition of finer sediments (clay and silt fraction) (Bridge, 2003;
 484 Fryirs & Brierley, 2013). However, the deposition of plastic particles also requires a reduced flow velocity because
 485 of the properties of the particles, especially their low density (Tibbetts *et al.*, 2018). Another explanation could be
 486 that more plastic particles are deposited in areas with increased accumulation of younger sediments take place
 487 (frequent flood activity and higher sediment accumulation at river banks). This explanation is supported by the low
 488 MP concentrations in active flood channel (STD-2, LIM-2), which might be caused by the erosion of the upper soil
 489 material and stored plastic particles inside. An explanation about land use and associated surface roughness
 490 (vegetation) also cannot be excluded (Klein *et al.*, 2015; Tibbetts *et al.*, 2018).

491
 492 In general, the differences between different land use classes and associated vegetation (riparian, cropland,
 493 grassland) are not distinct (Figure 5a). Even though the "riparian" class with a median of 2.45 mp/kg^{-1} is clearly
 494 above the concentrations of cropland (median 0.37 mp/kg^{-1}) and grassland (median 0.48 mp/kg^{-1}), this can be
 495 attributed to the increased concentrations in the area near the river banks (especially site LIM-1). Comparable to the
 496 results for larger plastic particles (MEP, CMP) (Weber & Opp, 2020), an accumulation of higher microplastic
 497 concentrations does not seem to occur in the area of intensive agricultural use (cropland). Although agriculture
 498 cannot be dismissed as a potential source of microplastics (e.g., from sources such as sewage sludge, compost,
 499 fertilizers, hay bale nets) (Corradini *et al.*, 2019; Braun *et al.*, 2021), the spatial position within the floodplain and
 500 the surface roughness caused by vegetation appear to be more important factors that can explain the lateral
 501 distribution of L-MP and M-MP particles.

502



503

504

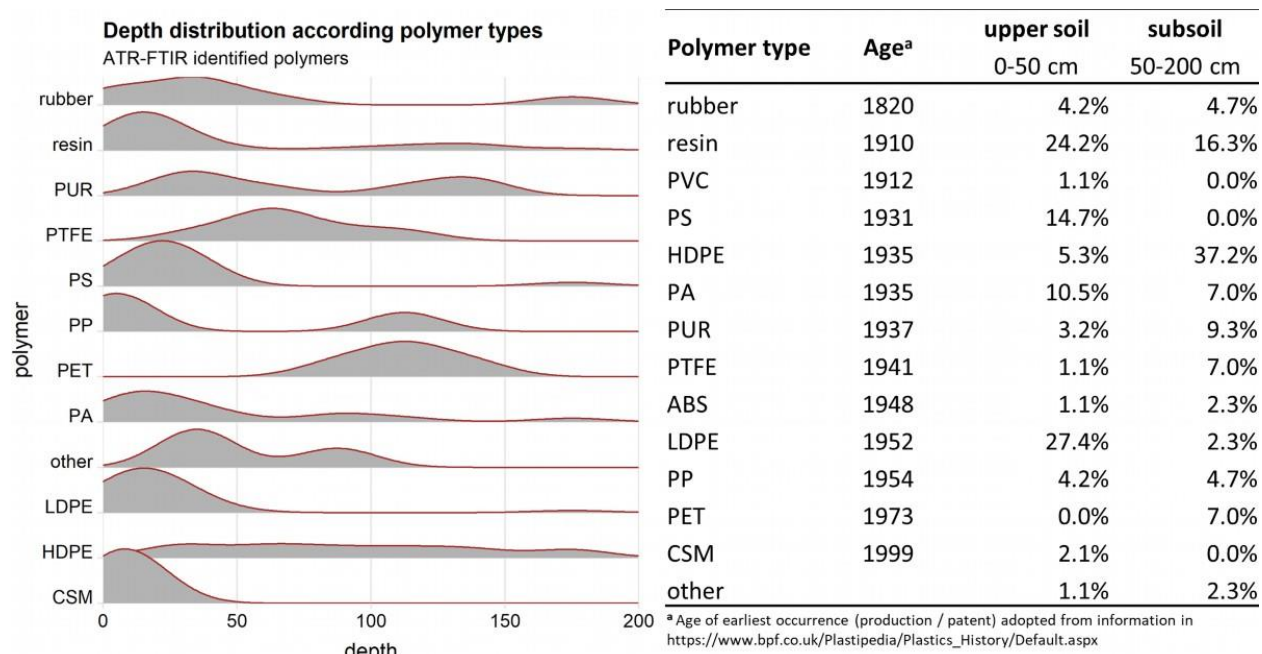
505 **Figure 5:** Microplastic distribution under different land use classes. (a) Total microplastic concentration (mp/kg)
 506 according to the land use classes. (b) Depth distribution (violin plot: boxplot with kernel density) of plastic concentrations
 507 (mean sample depth in cm) with medium tillage depth (plough tillage, for recent and relict soil horizons) by dotted
 508 line.

509 3.3 Vertical microplastic dynamics

510 The consideration of vertical microplastic distribution within floodplain soils as a three-dimensional system provides
 511 important information and enables understanding of vertical microplastic dynamics. With the exception of the study
 512 by Lechthaler *et al.* (2021), microplastics have never been searched for at soil depths up to 2 meters until now. If
 513 the depth of the floodplain soils is differentiated according to soil horizons, then the higher contents are clearly
 514 located in the topsoil horizons (represent A horizons) with average values of 3.33 mp/kg^{-1} higher than in the subsoil
 515 horizons (e.g., B) with 1.34 mp/kg^{-1} (Figure 1b, Table T1). Independent of the soil stratigraphy, the upper 50 cm
 516 (corresponding to 5 samples from one drill core) of the floodplain soils contain 67.65% of the identifiable plastic,
 517 whereas the depth range 50 to 200 cm (also 5 samples from one drill core) contains only 32.35% (Figure 2). With
 518 the exception of filaments, only particles with a size $< 2,000 \mu\text{m}$ occur in depths greater than 125 cm. The median

519 particle size within the upper 50 cm lies at 1,421.5 μm with major particle types of fragments, films, and filaments,
 520 whereas within the lower 150 cm the median particle size is slightly smaller with 1,301.0 μm (films and fragments,
 521 less filaments). Considering the depth distribution in relation to land use (Figure 5b), the depth distribution is
 522 basically comparable, even if in the riparian area depths > 150 cm are only reached in a few single cases. Median
 523 depth distribution is 35 cm for riparian and cropland and 62.5 for grassland, where it becomes clear that, under
 524 grassland, significantly deeper depths are also reached. The vertical distribution at the sampling site level is
 525 independent of this. The greatest depths (150-200 cm) are reached at sites ROT (proximal floodplain) and STD
 526 (proximal and distal floodplain). The two deepest depths (125-150 cm) are at sites LIM (proximal floodplain) and
 527 ROT (proximal floodplain). Particles therefore reach depths of up to a maximum of 2 meters, regardless of the
 528 distance to the watercourse, the soil type, or land use. Significant correlations, neither superordinate nor site specific
 529 between depth distribution and soil parameters (e.g., grain size, bulk density, OM, root distribution), could not be
 530 found (examples given in Figure S8). This and the occurrence of zero-values (empty samples), by unidentified
 531 particles but also by no particles found, indicates a clearly heterogeneous depth distribution starting at 50 cm depth,
 532 whereas a more homogeneous distribution can be assumed in the upper soil areas (0–50 cm).
 533

534 This also applies to the vertical distribution of polymer types and associated age of earliest possible occurrence
 535 (EPO age). Vertical structuring of floodplain soils is most commonly related to depositional history (sediment
 536 deposition), which is related to sedimentation rates (Brigde, 2003). Floodplain chronology can be assessed by
 537 different methods, as well as by plastics themselves. Since the global plastic productions started its exponential
 538 growth within the 1950s, plastics within floodplain soils could act as a new marker of floodplain chronology
 539 (Lechthaler *et al.*, 2021). For each identified polymer type, the EPO age can be added, based on the production
 540 starting year or year of patent registration (Weber & Opp, 2020; Lechthaler *et al.*, 2021). Based on the EPO age,
 541 each polymer can be used as a specific marker for the time between 1910 and 1990. From Figure 6, it becomes clear
 542 that the depth distribution of different polymer types is not equal over the depth. 71% of identified polymers
 543 including resins, LDPE, PS, and PA show a peak within the upper 50 cm of floodplain soils. Only HDPE, the third-
 544 most frequent polymer, shows an equal distribution over the depth. Assuming that polymers that have been released
 545 into the environment for a long time (e.g., rubber, resin, PVC with EPO ages < 1912) are found more frequently at
 546 deeper layers than "younger polymers" (EPO age > 1950), this should be reflected in the vertical distribution (Figure
 547 6). In fact, this is only achieved for very young polymers such as chlorosulfonated polyethylene (CSM, EPO age:
 548 1990s). All other polymers do not show a clear superordinate separation but also a heterogeneous distribution over
 549 the depth.
 550
 551

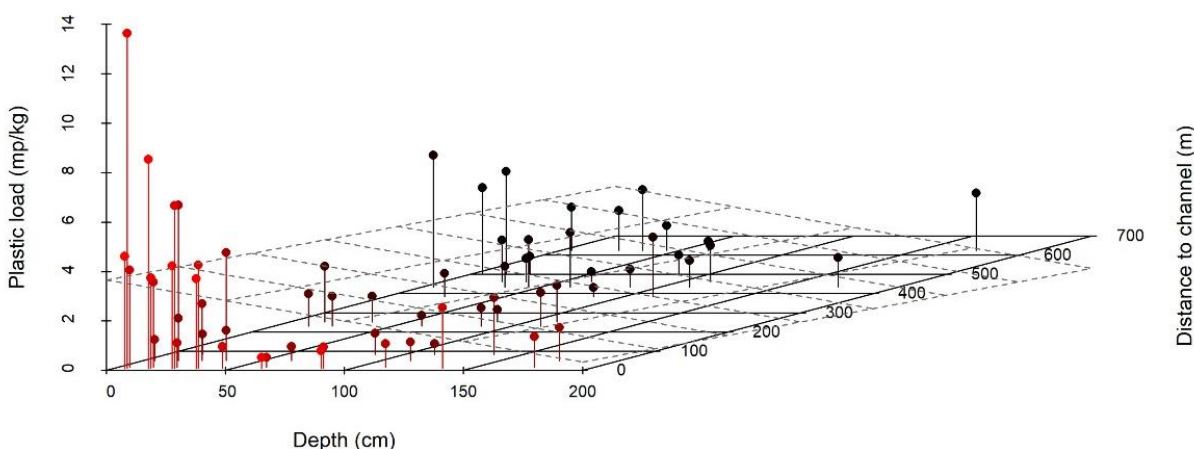


552
 553 **Figure 6.** Depth distribution of different identified polymer types and occurrence of different polymer types (sorted
 554 by age, production start, or patent submission) in upper and lower soil areas.

555
 556 The vertical distribution of the MP particles in combination with the evaluation of the EPO age-based depth
 557 distribution, underlines the clear separation into two parts: a) The upper floodplain soil area (approx. 0–50 cm) with
 558 a clear MP accumulation and the occurrence of very young polymer types as well as the b) lower soil area (approx.
 559 50-200 cm) with partwise MP occurrence, individual hotspots and mixed occurrence of different EPO ages

560 3.4 Reconstruction of microplastic deposition and translocation

561 Information on lateral and vertical MP distribution within floodplains soils in combination with derived EPO age
 562 and other soil parameters allows a first holistic assessment of the deposition conditions of microplastics in
 563 floodplains based on a geospatial sampling approach. Summarizing the spatial distribution, it can be stated that a
 564 clear concentration of increased MP occurrences can be found in the area of the proximal floodplain (i.e., the upper
 565 50 cm of the floodplain soil; Figure 7). Areal regression shows a clear decrease in MP content with increasing depth
 566 and a decrease with distance from the watercourse (distal floodplain), although individual hotspots occur near the
 567 surface.
 568

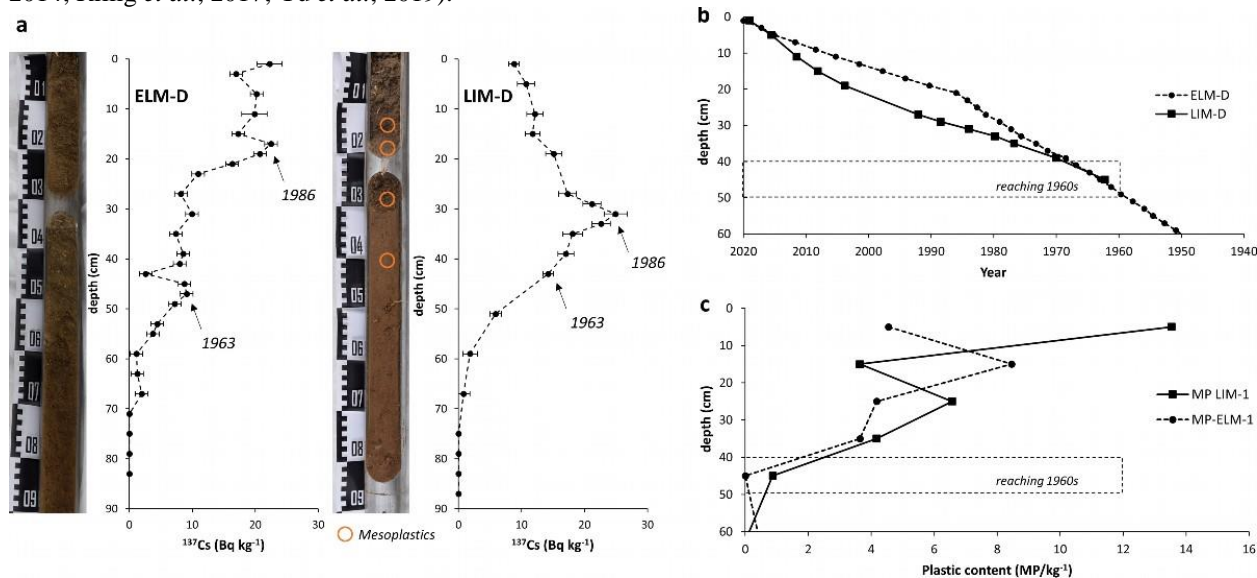


569
 570 **Figure 7.** Spatial representation of total microplastic loads (mp/kg) by depth (cm) and distance from the channel
 571 (m). Grey area (dotted lines): Regression area of combined concentrations. Color scale of pins ranging from red
 572 (proximal floodplain) to black (distal floodplain) based on distance to channel (m).
 573

574 The areal regression (Figure 7) indicates a dependence on MP inputs on the metric factors (a) depth in the soil
 575 profile and (b) distance to the watercourse. Because no dependence on other soil parameters or anthropogenic
 576 parameters (e.g., bulk density, land use, proximity to transport routes) could be proven, the MP input seems to be
 577 mainly attributable to floods as a transport medium because they reach areas near the banks more frequently than
 578 more distant ones. To examine this relationship, the question arises concerning the exact age of the sediments,
 579 especially the enrichment layer (0–50 cm). From both dating cores (ELM-D: upper course, LIM-D: lower course), it
 580 was possible to achieve sufficient results through the ^{210}Pb and ^{137}Cs dating. In case of the radionuclide ^{210}Pb , both
 581 cores show a steady concentration increase the closer to the soil surface (Figure S9). ELM-D shows an average ^{210}Pb
 582 concentration of 40.76 Bq kg^{-1} (0–90 cm) with a maximum concentration of 62.36 Bq kg^{-1} in the section 0-2 cm and
 583 an increase within the upper 20 cm of sampling core. Comparable concentrations are also found in the LIM-D core
 584 with an average ^{210}Pb concentration of 53.33 Bq kg^{-1} (0–90 cm) and maximum concentration of 82.93 Bq kg^{-1} in the
 585 section 4-6 cm. The analyses of ^{137}Cs concentrations enables the identification of concentration increases or peaks
 586 related to the atomic bomb tests of the 1950s to '60s (increase or peak in 1963) and the entry due to the Chernobyl
 587 nuclear disaster in 1986 (peak) (Andersen, 2017). A significant increase in ^{137}Cs concentrations can be observed for
 588 core ELM-D from 55 cm depth (first peak: 47 cm with 9.11 Bq kg^{-1} , second peak: 17 cm with 22.50 Bq kg^{-1}) and for
 589 core LIM-D from 51 cm depth (first increase: 43 cm with 14.23 Bq kg^{-1} , peak: 31 cm with 24.91 Bq kg^{-1}) (Figure
 590 8a). Based on the dating results, it can be concluded that near channel floodplain sediments were deposited within
 591 the 1960s at depths between 40 to 50 cm (Figure 8b). Calculated sedimentation rates related to the period between
 592 1986 and 2020 (34 years) show an average sedimentation rate of 0.5 cm/year for the upper reaches of the Lahn River
 593 (ELM-D) and 0.91 cm/a for the lower reaches (LIM-D), significantly higher than the catchment area rates (Lang &

594 Nolte, 1999; Rittweger, 2000; Martin, 2015; Weber & Opp, 2020). Finally, it can be concluded that the sediment age
 595 reaching the 1960s at a depth of 50 cm correspondence clearly with the increase of MP concentrations (Figure 8c).
 596

597 Combining the findings of lateral and vertical MP distribution with the dating results, it becomes even clearer that
 598 MPs are deposited in floodplain soils through sedimentation, with the increase in global production in the 1950s
 599 (exponential growth) (Andrady, 2017; PlasticsEurope, 2018, 2020). Because plastics were only used on a small scale
 600 before the 1950s, based on the dating results, the underlying plastic particles (> 50 cm) cannot have reached these
 601 depths by natural deposition but only by in-situ transport (e.g., preferential flow, bioturbation) (van Schaik *et al.*,
 602 2014; Rillig *et al.*, 2017; Yu *et al.*, 2019).



603
 604
 605 **Figure 8.** Sediment dating results. (a) ^{137}Cs (Bq kg⁻¹) concentrations for dating cores ELM-D and LIM-D with
 606 mesoplastic occurrence within core LIM-D (further information on soil density and ^{210}Pb content is given in Figure
 607 S9). (b) Calculated sediment ages (years) related to sediment depth (cm) for dating cores ELM-D and LIM-D. (c)
 608 Plastic content (mp/kg⁻¹) related to sampling depth for sampling sites ELM-1 and LIM-1 (upper 60 cm, plastic
 609 content below ranging from ELM-1: 0.72 mp/kg⁻¹, LIM-1: 0.85 to 2.45 mp/kg⁻¹) corresponding to dating cores.
 610

611 Finally, it can be concluded that a reconstruction of MP deposition and translocation in floodplain soils, based on the
 612 holistic research approach, can become qualitatively feasible (Figure 9). MP particles can reach the floodplain area
 613 through different input pathways, whereas the flood water delivery seems to play a major role. Accumulation of MP
 614 within young sediments (since 1960s) at near river sections (riparian zone, proximal floodplain) indicates floods as a
 615 key environmental driver because only those floodplain areas are reached regularly by floods and sediment
 616 deposition (Huggett, 2007; Martin, 2012). The lower and more heterogeneous occurrences of plastic in the
 617 remaining part of the floodplain also indicate a strong transport mechanism of floodwater because only flood water
 618 reaches the floodplain at times over a wide area (Bridge, 2003). Nevertheless, besides this accumulation since the
 619 1960, however, relocation processes must occur within the soil (Weber & Opp, 2020). Only in-situ relocations can
 620 explain the MP occurrences down to depths of 150 to 200 cm (sediments older than increase in global plastic
 621 production) because they cannot be pure depositional processes. Although displacement through the pore space of
 622 the soil is conceivable, the grain size analyses in this study show the widespread presence of loams (average
 623 contents: 19.64% clay, 48.03% silt, 32.22% sand) with a medium pore volume, a displacement of comparatively
 624 large particles can take place only through macropores (van Schaik *et al.*, 2014). Further possible processes that
 625 could be involved in a relocation and that are limited by the size of the particles (average of 1,171.04 μm) can be
 626 flow paths (preferential) or disturbances of the soil structure (corridors, bioturbation) (Rillig *et al.*, 2017; Hüffer *et*
 627 *al.*, 2019; Yu *et al.*, 2019; Hartmann *et al.*, 2020).
 628

629 In conclusion, MP (a) accumulates in floodplain soils on the one hand and (b) is translocated on the other. Thus,
 630 there is also a distinction between a more immobile MP fraction and more mobile MP fraction (particles < 2000
 631 μm), which can reach the deeper soil layers.

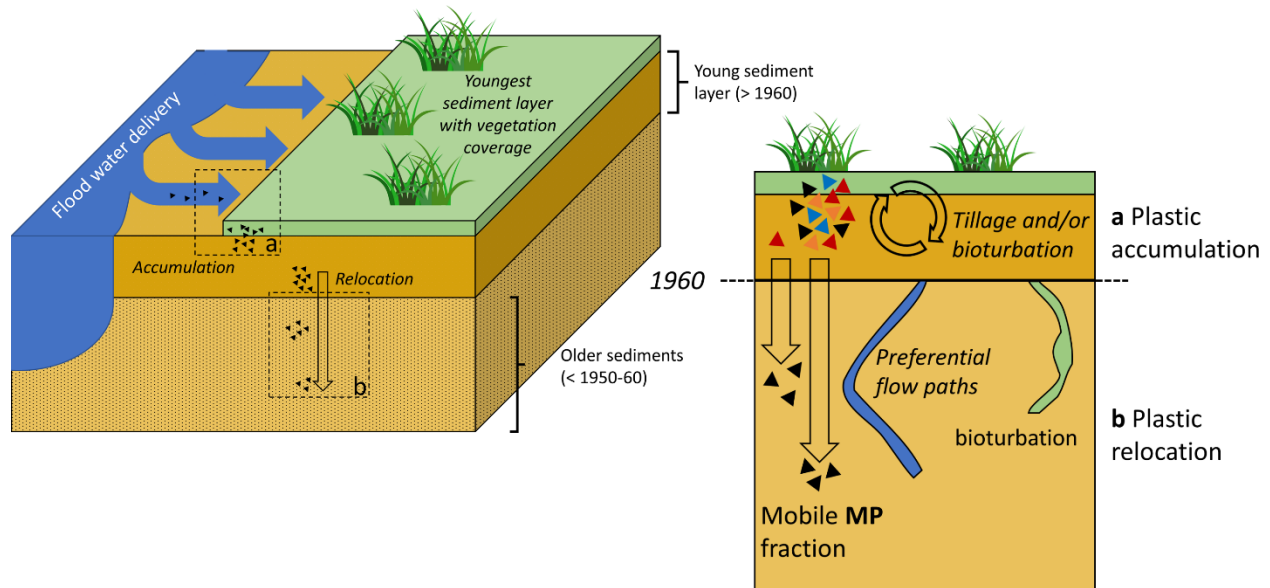


Figure 9. Scheme of MP deposition and redistribution in floodplain soils.

4 Conclusions

The spatial evidence of MP in floodplain soils and thus within the semiterrestrial system (aquatic-terrestrial interface) and its sediments illustrates that MP have become part of the sedimentary transport and thus simultaneously of the geological cycle within the Anthropocene. The heterogeneous but widespread distribution of plastic particles of different size classes, including MEP and CMP (Weber & Opp, 2020), in combination with the evidence from other studies in floodplain soils or freshwater systems in general, underlines this finding. The significant accumulation of MP in young sediments between 0 and 50 cm depth (deposition after 1960), which clearly corresponds to the increase in global plastic production, suggests that floodplains can act as a sink for microplastics. The temporal dimension highlights that plastic can, in principle, act as a stratigraphic marker of sediments in the Anthropocene, as suggested before (Price et al., 2011; Zalasiewicz et al., 2016; De-la-Torre et al., 2021). However, the pure occurrence of plastic cannot represent a specific marker because vertical displacement processes (mobile fraction < 2,000 μm , correspondence to CMP border) are possible.

Even if the consequences of plastic contamination in soils and sediments for different ecosystems are still under investigation and discussion, the widespread occurrence and accumulation of plastic alone should give cause for reflection. Plastic as a purely anthropogenic material without a natural equivalent and long residence times (Zalasiewicz et al., 2016; Chamas et al., 2020) has no place in the environment, especially not in global material cycles such as that of sediments. Humans influence the environment, and thus the future of the Earth, in manifold ways. Plastic should be understood as part of this influence and, against this backdrop, should be researched with a much stronger spatial focus. For further research on plastic and MP in floodplains, and in the semiterrestrial system in general, we recommend the following priorities:

1. **Spatial quantification:** In the context of a global plastic cycle, the representative spatial quantification of plastic and MP amounts in soils and sediments must be expanded. More data is needed to better understand and model plastic fluxes in the environment in the future.
2. **Environmental drivers:** Processes for understanding the mobility and displacement (lateral and vertical) of MP in soils and sediments should be analyzed in more detail. This analysis can be done in laboratory experiments (e.g., pot experiments), as well as in the field (e.g., pore characteristics, tracer experiments with plastic themselves or common tracers). The aim should be to understand the site-dependent key processes for MP mobility and to assess the resulting risks for the environment.
3. **Stratigraphic relevance:** Plastics and microplastics could play an important role in accessing the stratigraphic records and changes within the Anthropocene. The fate of plastics, not only as a stratigraphic

668 marker in floodplains, but also within different soils (especially anthropogenic soils), should be further
 669 investigated. In particular, the mobility of MP particles in soils could limit the use of MP as a marker,
 670 whereas larger plastic particles with lower mobility (MEP) could be used. Combinations with or extensions
 671 of available dating methods should be proofed.

672 **Acknowledgments, Samples, and Data**

673 **Funding:** This work was funded by the Hessian Agency of Nature Conservation, Environment and Geology (Hesse,
 674 Germany), and PhD Scholarship from the Marburg University Research Academy (MARA).

675
 676 **Acknowledgments:** The authors acknowledge support by all landowners who granted access to their land. We thank
 677 Alexander Santowski for his assistance during fieldwork.

678
 679 **Author Contributions:** Conceptualization, C.J.W. and C.O.; Methodology, C.J.W., J.A.P. and T.J.A.; Validation,
 680 C.J.W. and T.J.A.; Formal Analyses, C.J.W. and T.J.A.; Investigation, C.J.W.; Resources, C.J.W., C.O., M.K., P.C.
 681 and T.J.A.; Data Curation, C.J.W. and T.J.A., Writing – Original Draft, C.J.W., Writing – Review & Editing,
 682 C.J.W., J.A.P., C.O., M.K., P.C. and T.J.A., Visualization, C.J.W.; Supervision, C.O., M.K. and P.C.; Project
 683 Administration, C.J.W.; Funding Acquisition, C.J.W. and C.O.

684
 685 **Conflicts of Interest:** The authors declare no conflict of interest.

686
 687 **Data Availability:** Data generated within the framework of this study can be freely accessed at Weber, Collin J.;
 688 Andersen, Thorbjørn Joest (2021), “Plastic and microplastics in floodplain soils of the Lahn River catchment
 689 (Hesse, Germany)”, Mendeley Data, V1, doi: 10.17632/m864xphyr4.1.

690

691 **References**

- 692 Ad-hoc AG Boden. 2005. *Bodenkundliche Kartieranleitung*, 5th edn. Schweizerbart, Stuttgart.
- 693 Alimi, O.S., Farner Budarz, J., Hernandez, L.M. & Tufenkji, N. 2018. Microplastics and Nanoplastics in Aquatic
 694 Environments: Aggregation, Deposition, and Enhanced Contaminant Transport. *Environmental science &*
 695 *technology*, **52**, 1704–1724. doi: 10.1021/acs.est.7b05559.
- 696 Andersen, T.J. 2017. Some Practical Considerations Regarding the Application of ²¹⁰Pb and ¹³⁷Cs Dating to
 697 Estuarine Sediments. In *Applications of Paleoenvironmental Techniques in Estuarine Studies* (ed. K.
 698 Weckström, K.M. Saunders, P.A. Gell & C.G. Skilbeck), pp. 121–140. Springer, Dodrecht.
- 699 Andrady, A.L. 2017. The plastic in microplastics: A review. *Marine pollution bulletin*, **119**, 12–22. doi:
 700 10.1016/j.marpolbul.2017.01.082.
- 701 Appleby, P.G. 2001. Chronostratigraphic techniques in recent sediments. In *Tracking environmental change using*
 702 *lake sediments. Volume 1: Basin analysis, coring and chronological techniques* (ed. Last, W. M. & J.P. Smol).
 703 Kluwer Academic Publishers, Netherlands.
- 704 Barnes, D.K.A., Galgani, F., Thompson, R.C. & Barlaz, M. 2009. Accumulation and fragmentation of plastic debris
 705 in global environments. *Philosophical transactions of the Royal Society of London. Series B, Biological*
 706 *sciences*, **364**, 1985–1998. doi: 10.1098/rstb.2008.0205.
- 707 Bläsing, M. & Amelung, W. 2018. Plastics in soil: Analytical methods and possible sources. *The Science of the total*
 708 *environment*, **612**, 422–435. doi: 10.1016/j.scitotenv.2017.08.086.
- 709 Blettler, M.C.M., Ulla, M.A., Rabuffetti, A.P. & Garello, N. 2017. Plastic pollution in freshwater ecosystems:
 710 macro-, meso-, and microplastic debris in a floodplain lake. *Environmental monitoring and assessment*, **189**,
 711 581. doi: 10.1007/s10661-017-6305-8.
- 712 Bos, J.A.A. & Urz, R. 2003. Late Glacial and early Holocene environment in the middle Lahn river valley (Hessen,
 713 central-west Germany) and the local impact of early Mesolithic people?pollen and macrofossil evidence.
 714 *Vegetation History and Archaeobotany*, **12**, 19–36. doi: 10.1007/s00334-003-0006-7.
- 715 Braun, M., Mail, M., Heyse, R. & Amelung, W. 2021. Plastic in compost: Prevalence and potential input into
 716 agricultural and horticultural soils. *The Science of the total environment*, **760**, 143335. doi:
 717 10.1016/j.scitotenv.2020.143335.
- 718 Bridge, J.S. 2003. *Rivers and Floodplains: Forms, Processes, and Sedimentary Record*, 1st edn. Blackwell, Malden.
- 719 Brierley, G.J. & Fryirs, K.A. 2007. *Geomorphology and River Management*. Blackwell, Malden.

- 720 Bundesministerium für Umwelt, Naturschutz und Reaktorsicherheit. 2009. *Auenzustandsbericht: Flussauen in*
721 *Deutschland* [accessed on 15 March 2021].
- 722 Carpenter, E.J. & Smith, K.L. 1972. Plastics on the Sargasso Sea Surface. *Science*, 1240–1243.
- 723 Chamas, A., Moon, H., Zheng, J., Qiu, Y., Tabassum, T. & Jang, J.H., et al. 2020. Degradation Rates of Plastics in
724 the Environment. *ACS Sustainable chemistry & engineering*, **8**, 3494–3511. doi:
725 10.1021/acssuschemeng.9b06635.
- 726 Cole, M., Lindeque, P., Halsband, C. & Galloway, T.S. 2011. Microplastics as contaminants in the marine
727 environment: a review. *Marine pollution bulletin*, **62**, 2588–2597. doi: 10.1016/j.marpolbul.2011.09.025.
- 728 Coppock, R.L., Cole, M., Lindeque, P.K., Queirós, A.M. & Galloway, T.S. 2017. A small-scale, portable method for
729 extracting microplastics from marine sediments. *Environmental pollution (Barking, Essex 1987)*, **230**, 829–837.
730 doi: 10.1016/j.envpol.2017.07.017.
- 731 Corradini, F., Meza, P., Eguluz, R., Casado, F., Huerta-Lwanga, E. & Geissen, V. 2019. Evidence of microplastic
732 accumulation in agricultural soils from sewage sludge disposal. *The Science of the total environment*, **671**, 411–
733 420. doi: 10.1016/j.scitotenv.2019.03.368.
- 734 Cowger, W., Gray, A., Hapich, H., Rochman, C., Lynch, J. & Primpke, S., et al. 2020. *Open Specy*.
- 735 De-la-Torre, G.E., Dioses-Salinas, D.C., Pizarro-Ortega, C.I. & Santillán, L. 2021. New plastic formations in the
736 Anthropocene. *The Science of the total environment*, **754**, 142216. doi: 10.1016/j.scitotenv.2020.142216.
- 737 Durner, W., Iden, S.C. & Unold, G. von. 2017. The integral suspension pressure method (ISP) for precise particle-
738 size analysis by gravitational sedimentation. *Water resources research*, **53**, 33–48.
- 739 Ellen MacArthur Foundation. 2017. *The new plastics economy: Rethinking the future of plastics & catalysing*
740 *action*. Ellen MacArthur Foundation, Cowes.
- 741 FAO. 2006. *Guidelines for soil description*, 4th ed. Food and Agriculture Organization of the United Nations, Rome.
- 742 Food and Agriculture Organization of the United Nations (FAO). 2015. *Healthy soils are the basis for healthy food*
743 *production. Fact sheet*.
- 744 Fryirs, K.A. & Brierley, G.J. 2013. *Geomorphic analysis of river systems: An approach to reading the landscape*.
745 Wiley, Chichester West Sussex UK, Hoboken NJ.
- 746 Gleim, W. & Opp, C. 2004. Hochwasser und Hochwasserschutz im Einzugsgebiet der Lahn. *Marburger*
747 *Geographische Schriften*, 214–229.
- 748 Hartmann, A., Semenova, E., Weiler, M. & Blume, T. 2020. Field observations of soil hydrological flow path
749 evolution over 10 millennia. *Hydrology and earth system sciences*, **24**, 3271–3288. doi: 10.5194/hess-24-3271-
750 2020.
- 751 Hessian Agency for Nature Conservation, Environment and Geology. 2020. *Digital Soil Cover Data 1:50,000 Hesse*
752 *(BFD50)*, Wiesbaden.
- 753 Hidalgo-Ruz, V., Gutow, L., Thompson, R.C. & Thiel, M. 2012. Microplastics in the marine environment: a review
754 of the methods used for identification and quantification. *Environmental science & technology*, **46**, 3060–3075.
755 doi: 10.1021/es2031505.
- 756 Houben, P. 2012. Sediment budget for five millennia of tillage in the Rockenberg catchment (Wetterau loess basin,
757 Germany). *Quaternary Science Reviews*, **52**, 12–23. doi: 10.1016/j.quascirev.2012.07.011.
- 758 Huerta Lwanga, E., Mendoza Vega, J., Ku Quej, V., Chi, J.d.L.A., Sanchez Del Cid, L. & Chi, C., et al. 2017. Field
759 evidence for transfer of plastic debris along a terrestrial food chain. *Scientific reports*, **7**, 14071. doi:
760 10.1038/s41598-017-14588-2.
- 761 Hüffer, T., Metzelder, F., Sigmund, G., Slawek, S., Schmidt, T.C. & Hofmann, T. 2019. Polyethylene microplastics
762 influence the transport of organic contaminants in soil. *The Science of the total environment*, **657**, 242–247. doi:
763 10.1016/j.scitotenv.2018.12.047.
- 764 Huggett, R., J. 2007. *Fundamentals of Geomorphology*, 2nd edn. Routledge, New York.
- 765 Hurley, R.R., Lusher, A.L., Olsen, M. & Nizzetto, L. 2018. Validation of a Method for Extracting Microplastics
766 from Complex, Organic-Rich, Environmental Matrices. *Environmental science & technology*, **52**, 7409–7417.
767 doi: 10.1021/acs.est.8b01517.
- 768 Imhof, H.K., Schmid, J., Niessner, R., Ivleva, N.P. & Laforsch, C. 2012. A novel, highly efficient method for the
769 separation and quantification of plastic particles in sediments of aquatic environments. *Limnology and*
770 *oceanography: Methods*, **10**, 524–537. doi: 10.4319/lom.2012.10.524.
- 771 IUSS Working Group. 2015. World reference base for soil resources 2014, update 2015: International soil
772 classification system for naming soils and creating legends for soil maps. *World Soil Resources Reports, FAO*.
- 773 Jung, M.R., Horgen, F.D., Orski, S.V., Rodriguez C, V., Beers, K.L. & Balazs, G.H., et al. 2018. Validation of ATR
774 FT-IR to identify polymers of plastic marine debris, including those ingested by marine organisms. *Marine*
775 *pollution bulletin*, **127**, 704–716. doi: 10.1016/j.marpolbul.2017.12.061.

- 776 Kalias, A.J., Merkt, J. & Wunderlich, J. 2003. Environmental changes during the Holocene climatic optimum in
777 central Europe - human impact and natural causes. *Quaternary science reviews*, 33–79. doi: 10.1016/S0277-
778 3791(02)00181-6.
- 779 Karbalaei, S., Hanachi, P., Walker, T.R. & Cole, M. 2018. Occurrence, sources, human health impacts and mitigation
780 of microplastic pollution. *Environmental science and pollution research*, 36046–36063. doi: 10.1007/s11356-
781 018-3508-7.
- 782 Klein, S., Worch, E. & Knepper, T.P. 2015. Occurrence and Spatial Distribution of Microplastics in River Shore
783 Sediments of the Rhine-Main Area in Germany. *Environmental science & technology*, **49**, 6070–6076. doi:
784 10.1021/acs.est.5b00492.
- 785 Konde, S., Ornik, J., Prume, J.A., Taiber, J. & Koch, M. 2020. Exploring the potential of photoluminescence
786 spectroscopy in combination with Nile Red staining for microplastic detection. *Marine pollution bulletin*, **159**,
787 111475. doi: 10.1016/j.marpolbul.2020.111475.
- 788 Kooi, M. & Koelmans, A.A. 2019. Simplifying Microplastic via Continuous Probability Distributions for Size,
789 Shape, and Density. *Environmental science & technology letters*, **6**, 551–557. doi: 10.1021/acs.estlett.9b00379.
- 790 Lahive, E., Walton, A., Horton, A.A., Spurgeon, D.J. & Svendsen, C. 2019. Microplastic particles reduce
791 reproduction in the terrestrial worm *Enchytraeus crypticus* in a soil exposure. *Environmental pollution (Barking,*
792 *Essex 1987)*, **255**, 113174. doi: 10.1016/j.envpol.2019.113174.
- 793 Lang, A. & Nolte, S. 1999. The chronology of Holocene alluvial sediments from the Wetterau, Germany, provided
794 by optical and 14C dating. *The holocene*, 207–214. doi: 10.1191/2F095968399675119300.
- 795 Lechthaler, S., Esser, V., Schüttrumpf, H. & Stauch, G. 2021. Why analysing microplastics in floodplains matters:
796 application in a sedimentary context. *Environmental science: processes & impacts*, **71**, 299. doi:
797 10.1039/D0EM00431F.
- 798 Lechthaler, S., Waldschläger, K., Stauch, G. & Schüttrumpf, H. 2020. The Way of Macroplastic through the
799 Environment. *Environments*, **7**, 73. doi: 10.3390/environments7100073.
- 800 Liu, H., Tang, L., Liu, Y., Zeng, G., Lu, Y. & Wang, J., et al. 2019. Wetland-a hub for microplastic transmission in
801 the global ecosystem. *Resources, conservation and recycling*, **142**, 153–154. doi:
802 10.1016/j.resconrec.2018.11.028.
- 803 Liu, M., Lu, S., Song, Y., Lei, L., Hu, J. & Lv, W., et al. 2018. Microplastic and mesoplastic pollution in farmland
804 soils in suburbs of Shanghai, China. *Environmental pollution (Barking, Essex 1987)*, **242**, 855–862. doi:
805 10.1016/j.envpol.2018.07.051.
- 806 Lorenzo-Navarro, J., Castrillon-Santana, M., Gomez, M., Herrera, A. & Marin-Reyes, P.A. 2018. Automatic
807 Counting and Classification of Microplastic Particles. *Proceedings of the 7th international conference on pattern*
808 *recognition, applications and methods (ICPRAM 2018)*, 646–652. doi: 10.5220/0006725006460652.
- 809 Machado, Anderson A. de Souza, Kloas, W., Zarfl, C., Hempel, S. & Rillig, M.C. 2018. Microplastics as an
810 emerging threat to terrestrial ecosystems. *Global change biology*, **24**, 1405–1416. doi: 10.1111/gcb.14020.
- 811 Martin, C.W. 2012. Recent changes in heavy metal contamination at near-channel positions of the Lahn River,
812 central Germany. *Geomorphology*, **139-140**, 452–459. doi: 10.1016/j.geomorph.2011.11.010.
- 813 Martin, C.W. 2015. Trace metal storage in recent floodplain sediments along the Dill River, central Germany.
814 *Geomorphology*, **235**, 52–62. doi: 10.1016/j.geomorph.2015.01.032.
- 815 Martin, C.W. 2019. Trace metal concentrations along tributary streams of historically mined areas, Lower Lahn and
816 Dill River basins, central Germany. *Catena*, **174**, 174–183. doi: 10.1016/j.catena.2018.11.008.
- 817 Meschede, M. & Warr, L.N. 2019. *The Geology of Germany: A Process-Oriented Approach*. Springer International
818 Publishing, Cham.
- 819 Möller, J.N., Löder, M.G.J. & Laforsch, C. 2020. Finding Microplastics in Soils: A Review of Analytical Methods.
820 *Environmental science & technology*, **54**, 2078–2090. doi: 10.1021/acs.est.9b04618.
- 821 Napper, I.E. & Thompson, R.C. 2019. Environmental Deterioration of Biodegradable, Oxo-biodegradable,
822 Compostable, and Conventional Plastic Carrier Bags in the Sea, Soil, and Open-Air Over a 3-Year Period.
823 *Environmental science & technology*, 4775–4783. doi: 10.1021/acs.est.8b06984.
- 824 Nardi, F., Annis, A., Di Baldassarre, G., Vivoni, E.R. & Grimaldi, S. 2019. GFPLAIN250m, a global high-
825 resolution dataset of Earth's floodplains. *Scientific data*, **6**, 180309. doi: 10.1038/sdata.2018.309.
- 826 Opp, C., Stach, J. & Hanschmann, G. 1993: Load on differently used soils by heavy metals within the highly
827 contaminated area of Bitterfeld (FRG). *Science of the total environment*, **134**, 141-150. doi: 10.1016/S0048-
828 9697(05)80013-0
- 829 Piehl, S., Leibner, A., Löder, M.G.J., Dris, R., Bogner, C. & Laforsch, C. 2018. Identification and quantification of
830 macro- and microplastics on an agricultural farmland. *Scientific reports*, **8**, 17950. doi: 10.1038/s41598-018-
831 36172-y.

- 832 PlasticsEurope. 2018. Plastics - the facts 2018: An analysis of European plastic production, demand and waste data.
833 *Plastic Europe*.
- 834 PlasticsEurope. 2020. Plastics - the facts 2020: An analysis of European plastic production, demand and waste data.
- 835 Price, S.J., Ford, J.R., Cooper, A.H. & Neal, C. 2011. Humans as major geological and geomorphological agents in
836 the Anthropocene: the significance of artificial ground in Great Britain. *Philosophical transactions. Series A,*
837 *Mathematical, physical, and engineering sciences*, **369**, 1056–1084. doi: 10.1098/rsta.2010.0296.
- 838 Pripcke, S., Lorenz, C., Rascher-Friesenhausen, R. & Gerdts, G. 2017. An automated approach for microplastics
839 analysis using focal plane array (FPA) FTIR microscopy and image analysis. *Analytical Methods*, **9**, 1499–
840 1511. doi: 10.1039/C6AY02476A.
- 841 Pripcke, S., Wirth, M., Lorenz, C. & Gerdts, G. 2018. Reference database design for the automated analysis of
842 microplastic samples based on Fourier transform infrared (FTIR) spectroscopy. *Analytical and bioanalytical*
843 *chemistry*, **410**, 5131–5141. doi: 10.1007/s00216-018-1156-x.
- 844 Ragusa, A., Svelato, A., Santacroce, C., Catalano, P., Notarstefano, V. & Carnevali, O., et al. 2021. Plasticenta: First
845 evidence of microplastics in human placenta. *Environment international*, **146**, 106274. doi:
846 10.1016/j.envint.2020.106274.
- 847 Regional Council Giessen. 2015. *Hochwasserrisikomanagementplan für das hessische Einzugsgebiet der Lahn*
848 *(Flood risk management plan)*. Regional Council Giessen, Giessen.
- 849 Rillig, M.C., Lehmann, A., Souza Machado, A.A. de & Yang, G. 2019. Microplastic effects on plants. *The New*
850 *phytologist*. doi: 10.1111/nph.15794.
- 851 Rillig, M.C., Ziersch, L. & Hempel, S. 2017. Microplastic transport in soil by earthworms. *Scientific reports*, **7**,
852 1362. doi: 10.1038/s41598-017-01594-7.
- 853 Rittweger, H. 2000. The “Black Floodplain Soil” in the Amöneburger Becken, Germany: a lower Holocene marker
854 horizon and indicator of an upper Atlantic to Subboreal dry period in Central Europe? *CATENA*, 143–164. doi:
855 10.1016/S0341-8162(00)00113-2.
- 856 Ruggero, F., Gori, R. & Lubello, C. 2020. Methodologies for Microplastics Recovery and Identification in
857 Heterogeneous Solid Matrices: A Review. *Journal of Polymers and the Environment*, **28**, 739–748. doi:
858 10.1007/s10924-019-01644-3.
- 859 Scheurer, M. & Bigalke, M. 2018. Microplastics in Swiss Floodplain Soils. *Environmental science & technology*,
860 **52**, 3591–3598. doi: 10.1021/acs.est.7b06003.
- 861 Selonen, S., Dolar, A., Jemec Kokalj, A., Skalar, T., Parramon Dolcet, L. & Hurley, R., et al. 2020. Exploring the
862 impacts of plastics in soil - The effects of polyester textile fibers on soil invertebrates. *The Science of the total*
863 *environment*, **700**, 134451. doi: 10.1016/j.scitotenv.2019.134451.
- 864 Siegfried, M., Koelmans, A.A., Besseling, E. & Kroeze, C. 2017. Export of microplastics from land to sea. A
865 modelling approach. *Water research*, **127**, 249–257. doi: 10.1016/j.watres.2017.10.011.
- 866 Stock, F., Kochleus, C., Baensch-Baltruschat, B., Brennholt, N. & Reifferscheid, G. 2019. Sampling techniques and
867 preparation methods for microplastic analyses in the aquatic environment - A review. *TrAC Trends in Analytical*
868 *Chemistry*, **113**, 84–92. doi: 10.1016/j.trac.2019.01.014.
- 869 Thomas, D., Schütze, B., Heinze, W.M. & Steinmetz, Z. 2020. Sample Preparation Techniques for the Analysis of
870 Microplastics in Soil—A Review. *Sustainability*, **12**, 9074. doi: 10.3390/su12219074.
- 871 Maes, T., Jessop, R., Wellner, N., Haupt, K. & Mayes, A. G. 2017. A rapid-screening approach to detect and
872 quantify microplastics based in fluorescent tagging with Nile Red. *Scientific reports*. doi: 10.1038/srep44501.
- 873 Tibbetts, J., Krause, S., Lynch, I. & Sambrook Smith, G. 2018. Abundance, Distribution, and Drivers of
874 Microplastic Contamination in Urban River Environments. *Water*, **10**, 1597. doi: 10.3390/w10111597.
- 875 van Schaik, L., Palm, J., Klaus, J., Zehe, E. & Schröder, B. 2014. Linking spatial earthworm distribution to
876 macropore numbers and hydrological effectiveness. *Ecohydrology*, **7**, 401–408. doi: 10.1002/eco.1358.
- 877 Waldschläger, K. & Schüttrumpf, H. 2019a. Effects of Particle Properties on the Settling and Rise Velocities of
878 Microplastics in Freshwater under Laboratory Conditions. *Environmental science & technology*, **53**, 1958–1966.
879 doi: 10.1021/acs.est.8b06794.
- 880 Waldschläger, K. & Schüttrumpf, H. 2019b. Erosion Behavior of Different Microplastic Particles in Comparison to
881 Natural Sediments. *Environmental Science & Technology*, **53**, 13219–13227. doi: 10.1021/acs.est.9b05394.
- 882 Weber, C.J. & Opp, C. 2020. Spatial patterns of mesoplastics and coarse microplastics in floodplain soils as
883 resulting from land use and fluvial processes. *Environmental pollution*, **267**, 115390. doi:
884 10.1016/j.envpol.2020.115390.
- 885 Weber, C.J., Weihrauch, C., Opp, C. & Chiffard, P. 2020. Investigating microplastic dynamics in soils: Orientation
886 for sampling strategies and sample pre-processing. *Land degradation & development*, 270–284. doi:
887 10.1002/ldr.3676.

- 888 Weihrauch, C. 2019. Dynamics need space – A geospatial approach to soil phosphorus' reactions and migration.
889 *Geoderma*, **354**, 113775. doi: 10.1016/j.geoderma.2019.05.025.
- 890 Willgoose, G. 2018. *Principles of Soilscape and Landscape Evolution*. Cambridge University Press, Cambridge.
- 891 Wright, S.L., Thompson, R.C. & Galloway, T.S. 2013. The physical impacts of microplastics on marine organisms:
892 a review. *Environmental pollution*, **178**, 483–492. doi: 10.1016/j.envpol.2013.02.031.
- 893 Xiong, X., Wu, C., Elser, J.J., Mei, Z. & Hao, Y. 2018. Occurrence and fate of microplastic debris in middle and
894 lower reaches of the Yangtze River - From inland to the sea. *The Science of the total environment*, **659**, 66–73.
895 doi: 10.1016/j.scitotenv.2018.12.313.
- 896 Yu, M., van der Ploeg, M., Lwanga, E.H., Yang, X., Zhang, S. & Ma, X., et al. 2019. Leaching of microplastics by
897 preferential flow in earthworm (*Lumbricus terrestris*) burrows. *Environmental chemistry*, **16**, 31. doi:
898 10.1071/EN18161.
- 899 Zalasiewicz, J., Waters, C.N., Ivar do Sul, J.A., Corcoran, P.L., Barnosky, A.D. & Cearreta, A., et al. 2016. The
900 geological cycle of plastics and their use as a stratigraphic indicator of the Anthropocene. *Anthropocene*, **13**, 4–
901 17. doi: 10.1016/j.ancene.2016.01.002.
- 902 Zhang, B., Yang, X., Chen, L., Chao, J., Teng, J. & Wang, Q. 2020. Microplastics in soils: a review of possible
903 sources, analytical methods and ecological impacts. *Journal of chemical technology & biotechnology*, **37**, 1045.
904 doi: 10.1002/jctb.6334.
- 905 Zhang, G.S. & Liu, Y.F. 2018. The distribution of microplastics in soil aggregate fractions in southwestern China.
906 *The Science of the total environment*, **642**, 12–20. doi: 10.1016/j.scitotenv.2018.06.004.
- 907 Zhang, G.S., Zhang, F.X. & Li, X.T. 2019. Effects of polyester microfibers on soil physical properties: Perception
908 from a field and a pot experiment. *The Science of the total environment*, **670**, 1–7. doi:
909 10.1016/j.scitotenv.2019.03.149.
- 910 Zink, T., Geyer, R. & Startz, R. 2018. Toward Estimating Displaced Primary Production from Recycling: A Case
911 Study of U.S. Aluminum. *Journal of industrial ecology*, **22**, 314–326. doi: 10.1111/jiec.12557.
- 912